

10. ELECTROWEAK MODEL AND CONSTRAINTS ON NEW PHYSICS

Revised November 2009 by J. Erler (U. Mexico) and P. Langacker (Institute for Advanced Study).

- 10.1 Introduction
- 10.2 Renormalization and radiative corrections
- 10.3 Low energy electroweak observables
- 10.4 W and Z boson physics
- 10.5 Precision flavor physics
- 10.6 Experimental results
- 10.7 Constraints on new physics

10.1. Introduction

The standard electroweak model (SM) is based on the gauge group [1] $SU(2) \times U(1)$, with gauge bosons W_μ^i , $i = 1, 2, 3$, and B_μ for the $SU(2)$ and $U(1)$ factors, respectively, and the corresponding gauge coupling constants g and g' . The left-handed fermion fields of the i^{th} fermion family transform as doublets $\Psi_i = \begin{pmatrix} \nu_i \\ \ell_i^- \end{pmatrix}$ and $\begin{pmatrix} u_i \\ d_i' \end{pmatrix}$ under $SU(2)$, where $d_i' \equiv \sum_j V_{ij} d_j$, and V is the Cabibbo-Kobayashi-Maskawa mixing matrix. (Constraints on V and tests of universality are discussed in Ref. 2 and in the Section on “The CKM Quark-Mixing Matrix”. The extension of the formalism to allow an analogous leptonic mixing matrix is discussed in the Section on “Neutrino Mass, Mixing, and Flavor Change”.) The right-handed fields are $SU(2)$ singlets. In the minimal model there are three fermion families and a single complex Higgs doublet $\phi \equiv \begin{pmatrix} \phi^+ \\ \phi^0 \end{pmatrix}$ which is introduced for mass generation.

After spontaneous symmetry breaking the Lagrangian for the fermion fields, ψ_i , is

$$\begin{aligned} \mathcal{L}_F = & \sum_i \bar{\psi}_i \left(i \not{\partial} - m_i - \frac{gm_i H}{2M_W} \right) \psi_i \\ & - \frac{g}{2\sqrt{2}} \sum_i \bar{\Psi}_i \gamma^\mu (1 - \gamma^5) (T^+ W_\mu^+ + T^- W_\mu^-) \Psi_i \\ & - e \sum_i q_i \bar{\psi}_i \gamma^\mu \psi_i A_\mu \\ & - \frac{g}{2 \cos \theta_W} \sum_i \bar{\psi}_i \gamma^\mu (g_V^i - g_A^i \gamma^5) \psi_i Z_\mu . \end{aligned} \tag{10.1}$$

$\theta_W \equiv \tan^{-1}(g'/g)$ is the weak angle; $e = g \sin \theta_W$ is the positron electric charge; and $A \equiv B \cos \theta_W + W^3 \sin \theta_W$ is the (massless) photon field. $W^\pm \equiv (W^1 \mp iW^2)/\sqrt{2}$ and $Z \equiv -B \sin \theta_W + W^3 \cos \theta_W$ are the massive charged and neutral weak boson fields,

2 10. Electroweak model and constraints on new physics

respectively. T^+ and T^- are the weak isospin raising and lowering operators. The vector and axial-vector couplings are

$$g_V^i \equiv t_{3L}(i) - 2q_i \sin^2 \theta_W, \quad (10.2a)$$

$$g_A^i \equiv t_{3L}(i), \quad (10.2b)$$

where $t_{3L}(i)$ is the weak isospin of fermion i (+1/2 for u_i and ν_i ; -1/2 for d_i and e_i) and q_i is the charge of ψ_i in units of e .

The second term in \mathcal{L}_F represents the charged-current weak interaction [3,4]. For example, the coupling of a W to an electron and a neutrino is

$$-\frac{e}{2\sqrt{2}\sin\theta_W} \left[W_\mu^- \bar{\nu} \gamma^\mu (1 - \gamma^5) \nu + W_\mu^+ \bar{e} \gamma^\mu (1 - \gamma^5) e \right]. \quad (10.3)$$

For momenta small compared to M_W , this term gives rise to the effective four-fermion interaction with the Fermi constant given (at tree level, *i.e.*, lowest order in perturbation theory) by $G_F/\sqrt{2} = g^2/8M_W^2$. CP violation is incorporated in the SM by a single observable phase in V_{ij} . The third term in \mathcal{L}_F describes electromagnetic interactions (QED), and the last is the weak neutral-current interaction.

In Eq. (10.1), m_i is the mass of the i^{th} fermion ψ_i . For the quarks these are the current masses. For the light quarks, as described in the note on ‘‘Quark Masses’’ in the Quark Listings, $\hat{m}_u = 2.5_{-1.0}^{+0.8}$ MeV, $\hat{m}_d = 5.0_{-1.5}^{+1.0}$ MeV, and $\hat{m}_s = 105_{-35}^{+25}$ MeV. These are running $\overline{\text{MS}}$ masses evaluated at the scale $\mu = 2$ GeV. (In this Section we denote quantities defined in the modified minimal subtraction ($\overline{\text{MS}}$) scheme by a caret; the exception is the strong coupling constant, α_s , which will always correspond to the $\overline{\text{MS}}$ definition and where the caret will be dropped.) For the heavier quarks we use QCD sum rule constraints [5] and recalculate their masses in each call of our fits to account for their direct α_s dependence. We find, $\hat{m}_c(\mu = \hat{m}_c) = 1.266_{-0.036}^{+0.031}$ GeV and $\hat{m}_b(\mu = \hat{m}_b) = 4.198 \pm 0.023$ GeV, with a correlation of 25%. The top quark ‘‘pole’’ mass, $m_t = 173.1 \pm 1.3$ GeV, is an average [6] of published and preliminary CDF and DØ results from run I and II. We are working, however, with $\overline{\text{MS}}$ masses in all expressions to minimize theoretical uncertainties, and therefore convert this result to the top quark $\overline{\text{MS}}$ mass,

$$\hat{m}_t(\mu = \hat{m}_t) = m_t \left[1 - \frac{4}{3} \frac{\alpha_s}{\pi} + \mathcal{O}(\alpha_s^2) \right],$$

using the three-loop formula [7]. This introduces an additional uncertainty which we estimate to 0.5 GeV (the size of the three-loop term). We are assuming that the kinematic mass extracted from the collider events corresponds within this uncertainty to the pole mass. Using the BLM optimized [8] version of the two-loop perturbative QCD formula [9] (as we did in previous editions of this *Review*) gives virtually identical results. Thus, we will use $m_t = 173.1 \pm 0.6$ (stat.) ± 1.1 (syst.) ± 0.5 (QCD) GeV $\approx 173.1 \pm 1.35$ GeV (together with $M_H = 117$ GeV) for the numerical values quoted in Sec. 10.2–Sec. 10.5. In the presence of right-handed neutrinos, Eq. (10.1) gives rise also to Dirac neutrino masses. The possibility of Majorana masses is discussed in the Section on ‘‘Neutrino Mass, Mixing, and Flavor Change’’.

H is the physical neutral Higgs scalar which is the only remaining part of ϕ after spontaneous symmetry breaking. The Yukawa coupling of H to ψ_i , which is flavor diagonal in the minimal model, is $gm_i/2M_W$. In non-minimal models there are additional charged and neutral scalar Higgs particles [10].

10.2. Renormalization and radiative corrections

The SM has three parameters (not counting the Higgs boson mass, M_H , and the fermion masses and mixings). A particularly useful set contains the Z mass, the fine structure constant, and the Fermi constant, which will be discussed in turn:

The Z boson mass, $M_Z = 91.1876 \pm 0.0021$ GeV, has been determined from the Z lineshape scan at LEP 1 [11].

The fine structure constant, $\alpha = 1/137.035999084(51)$, is currently best determined from the e^\pm anomalous magnetic moment [12] using the revised 4-loop QED result from Ref. 13. (For other determinations, see Ref. 14.) In most electroweak renormalization schemes, it is convenient to define a running α dependent on the energy scale of the process, with $\alpha^{-1} \sim 137$ appropriate at very low energy, *i.e.* close to the Thomson limit. (The running has also been observed [15] directly.) For scales above a few hundred MeV this introduces an uncertainty due to the low energy hadronic contribution to vacuum polarization. In the modified minimal subtraction ($\overline{\text{MS}}$) scheme [16] (used for this *Review*), and with $\alpha_s(M_Z) = 0.120$ for the QCD coupling at M_Z , we have $\hat{\alpha}(m_\tau)^{-1} = 133.444 \pm 0.015$ and $\hat{\alpha}(M_Z)^{-1} = 127.916 \pm 0.015$. The latter corresponds to a quark sector contribution (without the top) to the conventional (on-shell) QED coupling, $\alpha(M_Z) = \frac{\alpha}{1 - \Delta\alpha(M_Z)}$, of $\Delta\alpha_{\text{had}}^{(5)}(M_Z) \approx 0.02793 \pm 0.00011$. These values are updated from Ref. 17 with $\Delta\alpha_{\text{had}}^{(5)}(M_Z)$ moved upwards and its uncertainty almost halved (mostly due to a more precise $\hat{m}_c(\hat{m}_c)$). Its correlation with the μ^\pm anomalous magnetic moment (see Sec. 10.5), as well as the non-linear α_s dependence of $\hat{\alpha}(M_Z)$ and the resulting correlation with the input variable α_s , are fully taken into account in the fits. This is done by using as actual input (fit constraint) instead of $\Delta\alpha_{\text{had}}^{(5)}(M_Z)$ the analogous low energy contribution by the three light quarks, $\Delta\alpha_{\text{had}}^{(3)}(1.8 \text{ GeV}) = (57.29 \pm 0.90) \times 10^{-4}$, and by calculating the perturbative and heavy quark contributions to $\hat{\alpha}(M_Z)$ in each call of the fits according to Ref. 17. The uncertainty is from e^+e^- annihilation data below 1.8 GeV and τ decay data; from isospin breaking effects (affecting the interpretation of the τ data); from uncalculated higher order perturbative and non-perturbative QCD corrections; and from the $\overline{\text{MS}}$ quark masses. Such a short distance mass definition (unlike the pole mass) is free from non-perturbative and renormalon [18] uncertainties. Various recent evaluations of $\Delta\alpha_{\text{had}}^{(5)}$ are summarized in Table 10.1. where the leading order relation between the $\overline{\text{MS}}$ and on-shell definitions is given by,

$$\Delta\hat{\alpha}(M_Z) - \Delta\alpha(M_Z) = \frac{\alpha}{\pi} \left(\frac{100}{27} - \frac{1}{6} - \frac{7}{4} \ln \frac{M_Z^2}{M_W^2} \right) \approx 0.0072,$$

4 10. Electroweak model and constraints on new physics

Table 10.1: Recent evaluations of the on-shell $\Delta\alpha_{\text{had}}^{(5)}(M_Z)$. For better comparison we adjusted central values and errors to correspond to a common and fixed value of $\alpha_s(M_Z) = 0.120$. References quoting results without the top quark decoupled are converted to the five flavor definition. Ref. [29] uses $\Lambda_{\text{QCD}} = 380 \pm 60$ MeV; for the conversion we assumed $\alpha_s(M_Z) = 0.118 \pm 0.003$.

Reference	Result	Comment
Martin, Zeppenfeld [19]	0.02744 ± 0.00036	PQCD for $\sqrt{s} > 3$ GeV
Eidelman, Jegerlehner [20]	0.02803 ± 0.00065	PQCD for $\sqrt{s} > 40$ GeV
Geshkenbein, Morgunov [21]	0.02780 ± 0.00006	$\mathcal{O}(\alpha_s)$ resonance model
Burkhardt, Pietrzyk [22]	0.0280 ± 0.0007	PQCD for $\sqrt{s} > 40$ GeV
Swartz [23]	0.02754 ± 0.00046	use of fitting function
Alemanly <i>et al.</i> [24]	0.02816 ± 0.00062	incl. τ decay data
Krasnikov, Rodenberg [25]	0.02737 ± 0.00039	PQCD for $\sqrt{s} > 2.3$ GeV
Davier & Höcker [26]	0.02784 ± 0.00022	PQCD for $\sqrt{s} > 1.8$ GeV
Kühn & Steinhauser [27]	0.02778 ± 0.00016	complete $\mathcal{O}(\alpha_s^2)$
Erler [17]	0.02779 ± 0.00020	conv. from $\overline{\text{MS}}$ scheme
Davier & Höcker [28]	0.02770 ± 0.00015	use of QCD sum rules
Groote <i>et al.</i> [29]	0.02787 ± 0.00032	use of QCD sum rules
Martin <i>et al.</i> [30]	0.02741 ± 0.00019	incl. new BES data
Burkhardt, Pietrzyk [31]	0.02763 ± 0.00036	PQCD for $\sqrt{s} > 12$ GeV
de Troconiz, Yndurain [32]	0.02754 ± 0.00010	PQCD for $s > 2$ GeV ²
Jegerlehner [33]	0.02765 ± 0.00013	conv. from MOM scheme
Hagiwara <i>et al.</i> [34]	0.02757 ± 0.00023	PQCD for $\sqrt{s} > 11.09$ GeV
Burkhardt, Pietrzyk [35]	0.02760 ± 0.00035	incl. KLOE data
Hagiwara <i>et al.</i> [36]	0.02770 ± 0.00022	incl. selected KLOE data
Jegerlehner [37]	0.02755 ± 0.00013	Adler function approach

and where the first term is from fermions and the other two are from W^\pm loops which are usually excluded from the on-shell definition. Most of the older results relied on $e^+e^- \rightarrow$ hadrons cross-section measurements up to energies of 40 GeV, which were somewhat higher than the QCD prediction, suggested stronger running, and were less precise. The most recent results typically assume the validity of perturbative QCD (PQCD) at scales of 1.8 GeV and above, and are in reasonable agreement with each other. (Evaluations in the on-shell scheme utilize threshold data from BES [38] as further input.) There is,

however, some discrepancy between analyzes based on $e^+e^- \rightarrow$ hadrons cross-section data and those based on τ decay spectral functions [39,40]. The latter utilize data from OPAL [41], CLEO [42], ALEPH [43], and Belle [44] and imply lower central values for the extracted M_H of about 6%. This discrepancy is smaller than in the past and at least some of it appears to be experimental. The dominant $e^+e^- \rightarrow \pi^+\pi^-$ cross-section was measured with the CMD-2 [45] and SND [46] detectors at the VEPP-2M e^+e^- collider at Novosibirsk and the results are (after an initial discrepancy due to a flaw in the Monte Carlo event generator used by SND) in good agreement with each other. As an alternative to cross-section scans, one can use the high statistics radiative return events at e^+e^- accelerators operating at resonances such as the Φ or the $\Upsilon(4S)$. The method [47] is systematic dominated. The BaBar collaboration [48] studied multi-hadron events radiatively returned from the $\Upsilon(4S)$, reconstructing the radiated photon and normalizing to $\mu^\pm\gamma$ final states. Their result is higher compared to VEPP-2M and in fact agrees quite well with the τ analysis including the energy dependence (shape). In contrast, the shape and smaller overall cross-section from the $\pi^+\pi^-$ radiative return results from the Φ obtained by the KLOE collaboration [49] differs significantly from what is observed by BaBar. The discrepancy originates from the kinematic region $\sqrt{s} \gtrsim 0.6$ GeV, and is most pronounced for $\sqrt{s} \gtrsim 0.85$ GeV. For a recent review on these e^+e^- data, see Ref. 50. All measurements including older data [51] are accounted for in the fits on the basis of results in Refs. [28,40,50]. Further improvement of this dominant theoretical uncertainty in the interpretation of precision data will require better measurements of the cross-section for $e^+e^- \rightarrow$ hadrons below the charmonium resonances including multi-pion and other final states. To improve the precisions in $\hat{m}_c(\hat{m}_c)$ and $\hat{m}_b(\hat{m}_b)$ it would help to remeasure the threshold regions of the heavy quarks as well as the electronic decay widths of the narrow $c\bar{c}$ and $b\bar{b}$ resonances.

The Fermi constant, $G_F = 1.166364(5) \times 10^{-5}$ GeV $^{-2}$, is derived from the muon lifetime formula*,

$$\tau_\mu^{-1} = \frac{G_F^2 m_\mu^5}{192\pi^3} F(\rho) \left(1 + \frac{3}{5} \frac{m_\mu^2}{M_W^2} \right) \left[1 + H_1(\rho) \frac{\hat{\alpha}(m_\mu)}{\pi} + H_2(\rho) \frac{\hat{\alpha}^2(m_\mu)}{\pi^2} \right], \quad (10.4)$$

where $\rho = m_e^2/m_\mu^2$, and where

$$\begin{aligned} F(\rho) &= 1 - 8\rho + 8\rho^3 - \rho^4 - 12\rho^2 \ln \rho = 0.999813, \\ H_1(\rho) &= \frac{25}{8} - \frac{\pi^2}{2} - \left(9 + 4\pi^2 + 12 \ln \rho \right) \rho \\ &\quad + 16\pi^2 \rho^{3/2} + \mathcal{O}(\rho^2) = -1.8079, \end{aligned}$$

* In the spirit of the Fermi theory, the propagator correction proportional to m_μ^2 could instead be incorporated into Δr (see below), but we choose to leave it in the definition of G_F for historical consistency.

6 10. Electroweak model and constraints on new physics

$$\begin{aligned}
 H_2(\rho) &= \frac{156815}{5184} - \frac{518}{81}\pi^2 - \frac{895}{36}\zeta(3) + \frac{67}{720}\pi^4 \\
 &+ \frac{53}{6}\pi^2 \ln 2 - \frac{5}{4}\pi^2\sqrt{\rho} + \mathcal{O}(\rho) = 6.7, \\
 \hat{\alpha}(m_\mu)^{-1} &= \alpha^{-1} + \frac{1}{3\pi} \ln \rho = 135.9 .
 \end{aligned}$$

The massless corrections to H_1 and H_2 have been obtained in Refs. 52 and 53, respectively. The mass corrections to H_1 have been known for some time [54], while those to H_2 are very recent [55]. Notice the term linear in m_e whose appearance was unforeseen and can be traced to the use of the muon pole mass in the prefactor [55]. The remaining uncertainty in G_F is experimental and has recently been halved by the MuLan [56] and FAST [57] collaborations.

With these inputs, $\sin^2 \theta_W$ and the W boson mass, M_W , can be calculated when values for m_t and M_H are given; conversely (as is done at present), M_H can be constrained by $\sin^2 \theta_W$ and M_W . The value of $\sin^2 \theta_W$ is extracted from Z pole observables and neutral-current processes [11,60], and depends on the renormalization prescription. There are a number of popular schemes [61–68] leading to values which differ by small factors depending on m_t and M_H . The notation for these schemes is shown in Table 10.2.

Table 10.2: Notations used to indicate the various schemes discussed in the text. Each definition of $\sin^2 \theta_W$ leads to values that differ by small factors depending on m_t and M_H . Approximate values are also given for illustration.

Scheme	Notation	Value
On-shell	s_W^2	0.2233
NOV	$s_{M_Z}^2$	0.2311
$\overline{\text{MS}}$	\hat{s}_Z^2	0.2313
$\overline{\text{MS}}$ ND	\hat{s}_{ND}^2	0.2315
Effective angle	\bar{s}_f^2	0.2316

- (i) The on-shell scheme [61] promotes the tree-level formula $\sin^2 \theta_W = 1 - M_W^2/M_Z^2$ to a definition of the renormalized $\sin^2 \theta_W$ to all orders in perturbation theory, *i.e.*, $\sin^2 \theta_W \rightarrow s_W^2 \equiv 1 - M_W^2/M_Z^2$:

$$M_W = \frac{A_0}{s_W(1 - \Delta r)^{1/2}} , \quad M_Z = \frac{M_W}{c_W} , \quad (10.5)$$

where $c_W \equiv \cos \theta_W$, $A_0 = (\pi\alpha/\sqrt{2}G_F)^{1/2} = 37.28061(8)$ GeV, and Δr includes the radiative corrections relating α , $\alpha(M_Z)$, G_F , M_W , and M_Z . One finds

10. Electroweak model and constraints on new physics 7

$\Delta r \sim \Delta r_0 - \rho_t / \tan^2 \theta_W$, where $\Delta r_0 = 1 - \alpha / \hat{\alpha}(M_Z) = 0.06655(11)$ is due to the running of α , and $\rho_t = 3G_F m_t^2 / 8\sqrt{2}\pi^2 = 0.00939(m_t/173.1 \text{ GeV})^2$ represents the dominant (quadratic) m_t dependence. There are additional contributions to Δr from bosonic loops, including those which depend logarithmically on M_H . One has $\Delta r = 0.0362 \mp 0.0005 \pm 0.00011$, where the second uncertainty is from $\alpha(M_Z)$. Thus the value of s_W^2 extracted from M_Z includes an uncertainty (∓ 0.00019) from the currently allowed range of m_t . This scheme is simple conceptually. However, the relatively large ($\sim 3\%$) correction from ρ_t causes large spurious contributions in higher orders.

- (ii) A more precisely determined quantity $s_{M_Z}^2$ [62] can be obtained from M_Z by removing the (m_t, M_H) dependent term from Δr [63], *i.e.*,

$$s_{M_Z}^2(1 - s_{M_Z}^2) \equiv \frac{\pi\alpha(M_Z)}{\sqrt{2}G_F M_Z^2}. \quad (10.6)$$

Using $\alpha(M_Z)^{-1} = 128.91 \pm 0.02$ yields $s_{M_Z}^2 = 0.23108 \mp 0.00005$. The small uncertainty in $s_{M_Z}^2$ compared to other schemes is because the m_t dependence has been removed by definition. However, the m_t uncertainty reemerges when other quantities (*e.g.*, M_W or other Z pole observables) are predicted in terms of M_Z .

Both s_W^2 and $s_{M_Z}^2$ depend not only on the gauge couplings but also on the spontaneous-symmetry breaking, and both definitions are awkward in the presence of any extension of the SM which perturbs the value of M_Z (or M_W). Other definitions are motivated by the tree-level coupling constant definition $\theta_W = \tan^{-1}(g'/g)$:

- (iii) In particular, the modified minimal subtraction ($\overline{\text{MS}}$) scheme introduces the quantity $\sin^2 \hat{\theta}_W(\mu) \equiv \hat{g}'^2(\mu) / [\hat{g}^2(\mu) + \hat{g}'^2(\mu)]$, where the couplings \hat{g} and \hat{g}' are defined by modified minimal subtraction and the scale μ is conveniently chosen to be M_Z for many electroweak processes. The value of $\hat{s}_Z^2 = \sin^2 \hat{\theta}_W(M_Z)$ extracted from M_Z is less sensitive than s_W^2 to m_t (by a factor of $\tan^2 \theta_W$), and is less sensitive to most types of new physics than s_W^2 or $s_{M_Z}^2$. It is also very useful for comparing with the predictions of grand unification. There are actually several variant definitions of $\sin^2 \hat{\theta}_W(M_Z)$, differing according to whether or how finite $\alpha \ln(m_t/M_Z)$ terms are decoupled (subtracted from the couplings). One cannot entirely decouple the $\alpha \ln(m_t/M_Z)$ terms from all electroweak quantities because $m_t \gg m_b$ breaks SU(2) symmetry. The scheme that will be adopted here decouples the $\alpha \ln(m_t/M_Z)$ terms from the γ - Z mixing [16,64], essentially eliminating any $\ln(m_t/M_Z)$ dependence in the formulae for asymmetries at the Z pole when written in terms of \hat{s}_Z^2 . (A similar definition is used for $\hat{\alpha}$.) The various definitions are related by

$$\hat{s}_Z^2 = c(m_t, M_H) s_W^2 = \bar{c}(m_t, M_H) s_{M_Z}^2, \quad (10.7)$$

where $c = 1.0361 \pm 0.0005$ and $\bar{c} = 1.0010 \mp 0.0002$. The quadratic m_t dependence is given by $c \sim 1 + \rho_t / \tan^2 \theta_W$ and $\bar{c} \sim 1 - \rho_t / (1 - \tan^2 \theta_W)$, respectively. The expressions for M_W and M_Z in the $\overline{\text{MS}}$ scheme are

$$M_W = \frac{A_0}{\hat{s}_Z(1 - \Delta\hat{r}_W)^{1/2}}, \quad M_Z = \frac{M_W}{\hat{\rho}^{1/2} \hat{c}_Z}, \quad (10.8)$$

8 10. Electroweak model and constraints on new physics

and one predicts $\Delta\hat{r}_W = 0.06971 \pm 0.00002 \pm 0.00011$. $\Delta\hat{r}_W$ has no quadratic m_t dependence, because shifts in M_W are absorbed into the observed G_F , so that the error in $\Delta\hat{r}_W$ is dominated by $\Delta r_0 = 1 - \alpha/\hat{\alpha}(M_Z)$ which induces the second quoted uncertainty. The quadratic m_t dependence has been shifted into $\hat{\rho} \sim 1 + \rho_t$, where including bosonic loops, $\hat{\rho} = 1.01047 \pm 0.00015$. Quadratic M_H effects are deferred to two-loop order, while the leading logarithmic M_H effect is a good approximation only for large M_H values which are currently disfavored by the precision data. As an illustration, the shift in M_W due to a large M_H (for fixed M_Z) is given by

$$\begin{aligned}\Delta_H M_W &= -\frac{11}{96} \frac{\alpha}{\pi} \frac{M_W}{c_W^2 - s_W^2} \ln \frac{M_H^2}{M_W^2} + \mathcal{O}(\alpha^2) \\ &\sim -200 \text{ MeV (for } M_H = 10 M_W).\end{aligned}$$

(iv) A variant $\overline{\text{MS}}$ quantity \hat{s}_{ND}^2 (used in the 1992 edition of this *Review*) does not decouple the $\alpha \ln(m_t/M_Z)$ terms [65]. It is related to \hat{s}_Z^2 by

$$\hat{s}_Z^2 = \hat{s}_{\text{ND}}^2 / \left(1 + \frac{\hat{\alpha}}{\pi} d\right), \quad (10.9a)$$

$$d = \frac{1}{3} \left(\frac{1}{\hat{s}^2} - \frac{8}{3} \right) \left[\left(1 + \frac{\alpha_s}{\pi}\right) \ln \frac{m_t}{M_Z} - \frac{15\alpha_s}{8\pi} \right], \quad (10.9b)$$

Thus, $\hat{s}_Z^2 - \hat{s}_{\text{ND}}^2 \sim -0.0002$ for $m_t = 173.1$ GeV.

(v) Yet another definition, the effective angle [66–68] \bar{s}_f^2 for the Z vector coupling to fermion f , is described in Sec. 10.3.

Experiments are at such level of precision that complete $\mathcal{O}(\alpha)$ radiative corrections must be applied. For neutral-current and Z pole processes, these corrections are conveniently divided into two classes:

1. QED diagrams involving the emission of real photons or the exchange of virtual photons in loops, but not including vacuum polarization diagrams. These graphs often yield finite and gauge-invariant contributions to observable processes. However, they are dependent on energies, experimental cuts, *etc.*, and must be calculated individually for each experiment.
2. Electroweak corrections, including $\gamma\gamma$, γZ , ZZ , and WW vacuum polarization diagrams, as well as vertex corrections, box graphs, *etc.*, involving virtual W and Z bosons. Many of these corrections are absorbed into the renormalized Fermi constant defined in Eq. (10.4). Others modify the tree-level expressions for Z pole observables and neutral-current amplitudes in several ways [58]. One-loop corrections are included for all processes. In addition, certain two-loop corrections are also important. In particular, two-loop corrections involving the top quark modify ρ_t in $\hat{\rho}$, Δr , and elsewhere by

$$\rho_t \rightarrow \rho_t [1 + R(M_H, m_t) \rho_t / 3]. \quad (10.10)$$

$R(M_H, m_t)$ is best described as an expansion in M_Z^2/m_t^2 . The unsuppressed terms were first obtained in Ref. 69, and are known analytically [70]. Contributions suppressed by M_Z^2/m_t^2 were first studied in Ref. 71 with the help of small and large Higgs mass expansions, which can be interpolated. These contributions are about as large as the leading ones in Refs. 69 and 70. The complete two-loop calculation of Δr (without further approximation) has been performed in Refs. 72 and 73 for fermionic and purely bosonic diagrams, respectively. Similarly, the electroweak two-loop calculation for the relation between \bar{s}_ℓ^2 and s_W^2 is complete [74] including the recently obtained purely bosonic contribution [75]. For M_H above its lower direct limit, $-17 < R \leq -13$.

Mixed QCD-electroweak contributions to gauge boson self-energies of order $\alpha\alpha_s m_t^2$ [76] and $\alpha\alpha_s^2 m_t^2$ [77] increase the predicted value of m_t by 6%. This is, however, almost entirely an artifact of using the pole mass definition for m_t . The equivalent corrections when using the $\overline{\text{MS}}$ definition $\hat{m}_t(\hat{m}_t)$ increase m_t by less than 0.5%. The subleading $\alpha\alpha_s$ corrections [78] are also included. Further three-loop corrections of order $\alpha\alpha_s^2$ [79], $\alpha^3 m_t^6$ [80,81], and $\alpha^2\alpha_s m_t^4$ (for $M_H = 0$) [80], are rather small. The same is true for $\alpha^3 M_H^4$ [82] corrections unless M_H approaches 1 TeV. Also known are the singlet contributions (pure gluonic intermediate states) of order $\alpha\alpha_s^2$ [83] and $\alpha\alpha_s^3$ [84]. Recently, the corresponding non-singlet contributions have been computed as well [85].

The leading electroweak two-loop terms for the $Z \rightarrow b\bar{b}$ -vertex of $\mathcal{O}(\alpha^2 m_t^4)$ have been obtained in Refs. 69 and 70, and the mixed QCD-electroweak contributions in Refs. 86 and 87. Very recently, the authors of Ref. 88 completed the two-loop electroweak fermionic corrections to \bar{s}_b^2 . The $\mathcal{O}(\alpha\alpha_s)$ -vertex corrections involving massless quarks [89] add coherently, resulting in a sizable effect and shift $\alpha_s(M_Z)$ when extracted from Z lineshape observables (see Sec. 10.3) by $\approx +0.0007$.

Throughout this *Review* we utilize electroweak radiative corrections from the program GAPP [90], which works entirely in the $\overline{\text{MS}}$ scheme, and which is independent of the package ZFITTER [68].

10.3. Low energy electroweak observables

It is convenient to write the four-fermion interactions relevant to ν -hadron, ν - e , as well as parity violating e -hadron and e - e neutral-current processes in a form that is valid in an arbitrary gauge theory (assuming massless left-handed neutrinos). One has,

$$\begin{aligned}
 -\mathcal{L}^{\nu h} = & \frac{G_F}{\sqrt{2}} \bar{\nu} \gamma^\mu (1 - \gamma^5) \nu \sum_i \left[\epsilon_L(i) \bar{q}_i \gamma_\mu (1 - \gamma^5) q_i \right. \\
 & \left. + \epsilon_R(i) \bar{q}_i \gamma_\mu (1 + \gamma^5) q_i \right], \tag{10.11}
 \end{aligned}$$

$$-\mathcal{L}^{\nu e} = \frac{G_F}{\sqrt{2}} \bar{\nu}_\mu \gamma^\mu (1 - \gamma^5) \nu_\mu \bar{e} \gamma_\mu (g_V^{\nu e} - g_A^{\nu e} \gamma^5) e, \tag{10.12}$$

10 10. Electroweak model and constraints on new physics

$$-\mathcal{L}^{eh} = -\frac{G_F}{\sqrt{2}} \sum_i \left[C_{1i} \bar{e} \gamma_\mu \gamma^5 e \bar{q}_i \gamma^\mu q_i + C_{2i} \bar{e} \gamma_\mu e \bar{q}_i \gamma^\mu \gamma^5 q_i \right], \quad (10.13)$$

$$-\mathcal{L}^{ee} = -\frac{G_F}{\sqrt{2}} C_{2e} \bar{e} \gamma_\mu \gamma^5 e \bar{e} \gamma^\mu e, \quad (10.14)$$

where one must include the charged-current contribution for ν_e - e and $\bar{\nu}_e$ - e and the parity-conserving QED contribution for electron scattering.

The SM expressions for $\epsilon_{L,R}(i)$, $g_{V,A}^{\nu e}$, and C_{ij} are given in Table 10.3. Note, that $g_{V,A}^{\nu e}$ and the other quantities are coefficients of effective four-Fermi operators, which differ from the quantities defined in Eq. (10.2) in the radiative corrections and in the presence of possible physics beyond the SM.

10.3.1. Neutrino scattering :

A precise determination of the on-shell s_W^2 , which depends only very weakly on m_t and M_H , is obtained from deep inelastic scattering (DIS) of neutrinos from (approximately) isoscalar targets [91]. The ratio $R_\nu \equiv \sigma_{\nu N}^{NC} / \sigma_{\nu N}^{CC}$ of neutral-to-charged-current cross-sections has been measured to 1% accuracy by the CDHS [92] and CHARM [93] collaborations at CERN. The CCFR [94] collaboration at Fermilab has obtained an even more precise result, so it is important to obtain theoretical expressions for R_ν and $R_{\bar{\nu}} \equiv \sigma_{\bar{\nu} N}^{NC} / \sigma_{\bar{\nu} N}^{CC}$ to comparable accuracy. Fortunately, many of the uncertainties from the strong interactions and neutrino spectra cancel in the ratio. A large theoretical uncertainty is associated with the c -threshold, which mainly affects σ^{CC} . Using the slow rescaling prescription [95] the central value of $\sin^2 \theta_W$ from CCFR varies as $0.0111(m_c [\text{GeV}] - 1.31)$, where m_c is the effective mass which is numerically close to the $\overline{\text{MS}}$ mass $\hat{m}_c(\hat{m}_c)$, but their exact relation is unknown at higher orders. For $m_c = 1.31 \pm 0.24$ GeV (determined from ν -induced dimuon production [96]) this contributes ± 0.003 to the total uncertainty $\Delta \sin^2 \theta_W \sim \pm 0.004$. (The experimental uncertainty is also ± 0.003 .) This uncertainty largely cancels, however, in the Paschos-Wolfenstein ratio [97],

$$R^- = \frac{\sigma_{\nu N}^{NC} - \sigma_{\bar{\nu} N}^{NC}}{\sigma_{\nu N}^{CC} - \sigma_{\bar{\nu} N}^{CC}}. \quad (10.15)$$

It was measured by Fermilab's NuTeV collaboration [98] for the first time, and required a high-intensity and high-energy anti-neutrino beam.

A simple zeroth-order approximation is

$$R_\nu = g_L^2 + g_R^2 r, \quad R_{\bar{\nu}} = g_L^2 + \frac{g_R^2}{r}, \quad R^- = g_L^2 - g_R^2, \quad (10.16)$$

where

$$g_L^2 \equiv \epsilon_L(u)^2 + \epsilon_L(d)^2 \approx \frac{1}{2} - \sin^2 \theta_W + \frac{5}{9} \sin^4 \theta_W, \quad (10.17a)$$

$$g_R^2 \equiv \epsilon_R(u)^2 + \epsilon_R(d)^2 \approx \frac{5}{9} \sin^4 \theta_W, \quad (10.17b)$$

Table 10.3: Standard Model expressions for the neutral-current parameters for ν -hadron, ν - e , and e^- -scattering processes. At tree level, $\rho = \kappa = 1$, $\lambda = 0$. If radiative corrections are included, $\rho_{\nu N} = 1.0081$, $\widehat{\kappa}_{\nu N}(\langle Q^2 \rangle = -20 \text{ GeV}^2) = 0.9972$, $\widehat{\kappa}_{\nu N}(\langle Q^2 \rangle = -35 \text{ GeV}^2) = 0.9964$, $\lambda_{uL} = -0.0031$, $\lambda_{dL} = -0.0025$ and $\lambda_R = 3.7 \times 10^{-5}$. For ν - e scattering, $\rho_{\nu e} = 1.0127$ and $\widehat{\kappa}_{\nu e} = 0.9965$ (at $\langle Q^2 \rangle = 0$). For atomic parity violation and the polarized DIS experiment at SLAC, $\rho'_e = 0.9877$, $\rho_e = 1.0006$, $\widehat{\kappa}'_e = 1.0026$, $\widehat{\kappa}_e = 1.0299$, $\lambda' = -1.8 \times 10^{-5}$, $\lambda_u = -0.0118$ and $\lambda_d = 0.0029$. And for polarized Møller scattering with SLAC (JLab) kinematics, $\lambda_e = -0.0002$ ($\lambda_e = -0.0004$). The dominant m_t dependence is given by $\rho \sim 1 + \rho_t$, while $\widehat{\kappa} \sim 1$ ($\overline{\text{MS}}$) or $\kappa \sim 1 + \rho_t / \tan^2 \theta_W$ (on-shell).

Quantity	Standard Model Expression
$\epsilon_L(u)$	$\rho_{\nu N} \left(\frac{1}{2} - \frac{2}{3} \widehat{\kappa}_{\nu N} \widehat{s}_Z^2 \right) + \lambda_{uL}$
$\epsilon_L(d)$	$\rho_{\nu N} \left(-\frac{1}{2} + \frac{1}{3} \widehat{\kappa}_{\nu N} \widehat{s}_Z^2 \right) + \lambda_{dL}$
$\epsilon_R(u)$	$\rho_{\nu N} \left(-\frac{2}{3} \widehat{\kappa}_{\nu N} \widehat{s}_Z^2 \right) + \lambda_R$
$\epsilon_R(d)$	$\rho_{\nu N} \left(\frac{1}{3} \widehat{\kappa}_{\nu N} \widehat{s}_Z^2 \right) + 2 \lambda_R$
$g_V^{\nu e}$	$\rho_{\nu e} \left(-\frac{1}{2} + 2 \widehat{\kappa}_{\nu e} \widehat{s}_Z^2 \right)$
$g_A^{\nu e}$	$\rho_{\nu e} \left(-\frac{1}{2} \right)$
C_{1u}	$\rho'_e \left(-\frac{1}{2} + \frac{4}{3} \widehat{\kappa}'_e \widehat{s}_Z^2 \right) + \lambda'$
C_{1d}	$\rho'_e \left(\frac{1}{2} - \frac{2}{3} \widehat{\kappa}'_e \widehat{s}_Z^2 \right) - 2 \lambda'$
C_{2u}	$\rho_e \left(-\frac{1}{2} + 2 \widehat{\kappa}_e \widehat{s}_Z^2 \right) + \lambda_u$
C_{2d}	$\rho_e \left(\frac{1}{2} - 2 \widehat{\kappa}_e \widehat{s}_Z^2 \right) + \lambda_d$
C_{2e}	$\rho_e \left(\frac{1}{2} - 2 \widehat{\kappa}_e \widehat{s}_Z^2 \right) + \lambda_e$

and $r \equiv \sigma_{\bar{\nu}N}^{CC} / \sigma_{\nu N}^{CC}$ is the ratio of $\bar{\nu}$ to ν charged-current cross-sections, which can be measured directly. (In the simple parton model, ignoring hadron energy cuts, $r \approx (\frac{1}{3} + \epsilon) / (1 + \frac{1}{3}\epsilon)$, where $\epsilon \sim 0.125$ is the ratio of the fraction of the nucleon's momentum carried by anti-quarks to that carried by quarks.) In practice, Eq. (10.16) must be corrected for quark mixing, quark sea effects, c -quark threshold effects, non-isoscalarity, W - Z propagator differences, the finite muon mass, QED and electroweak radiative corrections. Details of the neutrino spectra, experimental cuts, x and Q^2 dependence of structure functions, and longitudinal structure functions enter only at the

12 10. Electroweak model and constraints on new physics

level of these corrections and therefore lead to very small uncertainties. The CCFR group quotes $s_W^2 = 0.2236 \pm 0.0041$ for $(m_t, M_H) = (175, 150)$ GeV with very little sensitivity to (m_t, M_H) .

The NuTeV collaboration found $s_W^2 = 0.2277 \pm 0.0016$ (for the same reference values), which was 3.0σ higher than the SM prediction [98]. Since then a number of experimental and theoretical developments implied shifts in the extracted s_W^2 , most of them reducing the discrepancy: (i) NuTeV also measured [99] the difference between the strange and antistrange quark momentum distributions, $S^- \equiv \int_0^1 dx x [s(x) - \bar{s}(x)] = 0.00196 \pm 0.00143$, from dimuon events utilizing the first complete next-to-leading order QCD description [100] and parton distribution functions (PDFs) according to Ref. 101. The magnitude of the central value agrees with the earlier result [102] but differs in sign. The effect of $S^- \neq 0$ on the NuTeV value for s_W^2 has been studied in Ref. 102, and the S^- above translates into a shift $\delta s_W^2 = -0.0014 \pm 0.0010$. On the other hand, there are theoretical arguments (see Ref. 103 and references therein) favoring a zero crossing of $x[s(x) - \bar{s}(x)]$ at values much larger than seen by NuTeV and suggesting an effect of much smaller and perhaps negligible size. We will therefore take half of the above shift as an estimate of both the S^- effect and the associated uncertainty, $\delta s_W^2 = -0.0007 \pm 0.0007$, replacing the original uncertainty [98] of ± 0.00047 . (ii) The measured branching ratio for K_{e3} decays enters crucially in the determination of the $\nu_e(\bar{\nu}_e)$ contamination of the $\nu_\mu(\bar{\nu}_\mu)$ beam. This branching ratio has moved from $4.82 \pm 0.06\%$ at the time of the original publication [98] to the current value of $5.07 \pm 0.04\%$, *i.e.*, a change by more than 4σ . To reflect this, we move s_W^2 by $+0.0016$ and reduce the $\nu_e(\bar{\nu}_e)$ uncertainty by a factor of $2/3$. (iii) PDFs seem to violate isospin symmetry at levels much stronger than generally expected [104]. A minimum χ^2 set of PDFs generalized in this sense [105,106] shows a reduction in the NuTeV discrepancy in s_W^2 by 0.0015 . But isospin symmetry violating PDFs are currently not well constrained phenomenologically and within uncertainties the NuTeV anomaly could be accounted for in full or conversely made larger [105]. Still, the leading contribution from quark mass differences turns out to be largely model-independent [107] and a shift, $\delta s_W^2 = -0.0015 \pm 0.0003$ [103], is applied. (iv) QED splitting effects also violate isospin symmetry with an effect on s_W^2 whose sign (reducing the discrepancy) is model-independent. The corresponding shift of $\delta s_W^2 = -0.0011$ has been calculated in Ref. 108 and a 100% uncertainty is assigned to it. (v) Nuclear shadowing effects [109] are likely to affect the interpretation of the NuTeV result at some level, but the NuTeV collaboration argues that their data are dominated by values of Q^2 at which nuclear shadowing is expected to be relatively small so that we do not apply a correction. However, another nuclear effect, the isovector EMC effect [110], is much larger (because it affects all neutrons in the nucleus, not just the excess ones) and model-independently works to reduce the discrepancy. It is estimated to lead to a shift of $\delta s_W^2 = -0.0019 \pm 0.0006$ [103]. (vi) The extracted s_W^2 may also shift at the level of the quoted uncertainty when analyzed using the most recent QED and electroweak radiative corrections [111,112], as well as QCD corrections to the structure functions [113]. However, their precise impact can be estimated only after the NuTeV data have been analyzed with a new set of PDFs including these new radiative corrections while simultaneously allowing isospin breaking and asymmetric strange seas. Remaining

one- and two-loop radiative corrections have been estimated [112] to induce uncertainties in the extracted s_W^2 of ± 0.0004 and ± 0.0003 , respectively, compared to the initial error of ± 0.00011 [102]. Most of the s_W^2 dependence and the NuTeV discrepancy reside in g_L^2 (initially 2.7σ low). Thus, the total shift of $\delta s_W^2 = -0.0036 \pm 0.0015$ corresponds to $\delta g_L^2 = +0.0027 \mp 0.0011$ and we arrive at $g_L^2 = 0.3027 \pm 0.0018$ which we use as a constraint in the fits. The right-handed coupling, $g_R^2 = 0.0308 \pm 0.0011$ (which is 0.7σ high) and the other ν -DIS data are expected to exhibit shifts as well, but these ought to be less significant since their relative experimental uncertainties are larger. In view of these developments and caveats, we use the NuTeV result in this *Review* but consider it along with the other ν -DIS data as preliminary until a re-analysis using PDFs including all experimental and theoretical information and correlations has been completed.

The cross-section in the laboratory system for $\nu_\mu e \rightarrow \nu_\mu e$ or $\bar{\nu}_\mu e \rightarrow \bar{\nu}_\mu e$ elastic scattering is

$$\frac{d\sigma_{\nu,\bar{\nu}}}{dy} = \frac{G_F^2 m_e E_\nu}{2\pi} \left[(g_V^{\nu e} \pm g_A^{\nu e})^2 + (g_V^{\nu e} \mp g_A^{\nu e})^2 (1-y)^2 - (g_V^{\nu e 2} - g_A^{\nu e 2}) \frac{y m_e}{E_\nu} \right], \quad (10.18)$$

where the upper (lower) sign refers to ν_μ ($\bar{\nu}_\mu$), and $y \equiv T_e/E_\nu$ (which runs from 0 to $(1 + m_e/2E_\nu)^{-1}$) is the ratio of the kinetic energy of the recoil electron to the incident ν or $\bar{\nu}$ energy. For $E_\nu \gg m_e$ this yields a total cross-section

$$\sigma = \frac{G_F^2 m_e E_\nu}{2\pi} \left[(g_V^{\nu e} \pm g_A^{\nu e})^2 + \frac{1}{3} (g_V^{\nu e} \mp g_A^{\nu e})^2 \right]. \quad (10.19)$$

The most accurate measurements [114–117] of $\sin^2 \theta_W$ from ν -lepton scattering are from the ratio $R \equiv \sigma_{\nu_\mu e} / \sigma_{\bar{\nu}_\mu e}$ in which many of the systematic uncertainties cancel. Radiative corrections (other than m_t effects) are small compared to the precision of present experiments and have negligible effect on the extracted $\sin^2 \theta_W$. The most precise experiment (CHARM II) [116] determined not only $\sin^2 \theta_W$ but $g_{V,A}^{\nu e}$ as well. The cross-sections for $\nu_e e$ and $\bar{\nu}_e e$ may be obtained from Eq. (10.18) by replacing $g_{V,A}^{\nu e}$ by $g_{V,A}^{\nu e} + 1$, where the 1 is due to the charged-current contribution [117,118].

10.3.2. *Parity violation :*

The SLAC polarized electron-deuteron DIS experiment [119] measured the right-left asymmetry,

$$A = \frac{\sigma_R - \sigma_L}{\sigma_R + \sigma_L}, \quad (10.20)$$

where $\sigma_{R,L}$ is the cross-section for the deep-inelastic scattering of a right- or left-handed electron: $e_{R,L} N \rightarrow eX$. In the quark parton model,

$$\frac{A}{Q^2} = a_1 + a_2 \frac{1 - (1-y)^2}{1 + (1-y)^2}, \quad (10.21)$$

14 10. Electroweak model and constraints on new physics

where $Q^2 > 0$ is the momentum transfer and y is the fractional energy transfer from the electron to the hadrons. For the deuteron or other isoscalar targets, one has, neglecting the s -quark and anti-quarks,

$$a_1 = \frac{3G_F}{5\sqrt{2}\pi\alpha} \left(C_{1u} - \frac{1}{2}C_{1d} \right) \approx \frac{3G_F}{5\sqrt{2}\pi\alpha} \left(-\frac{3}{4} + \frac{5}{3}\sin^2\theta_W \right), \quad (10.22a)$$

$$a_2 = \frac{3G_F}{5\sqrt{2}\pi\alpha} \left(C_{2u} - \frac{1}{2}C_{2d} \right) \approx \frac{9G_F}{5\sqrt{2}\pi\alpha} \left(\sin^2\theta_W - \frac{1}{4} \right). \quad (10.22b)$$

In another polarized-electron scattering experiment on deuterons, but in the quasi-elastic kinematic regime, the SAMPLE experiment [120] at MIT-Bates extracted the combination $C_{2u} - C_{2d}$ at Q^2 values of 0.1 GeV² and 0.038 GeV². What was actually determined were nucleon form factors from which the quoted results were obtained by the removal of a multi-quark radiative correction [121]. Other linear combinations of the C_{iq} have been determined in polarized-lepton scattering at CERN in μ -C DIS, at Mainz in e -Be (quasi-elastic), and at Bates in e -C (elastic). See the review articles in Refs. 59 and 122 for more details. Recent polarized electron asymmetry experiments, *i.e.*, SAMPLE, the PVA4 experiment at Mainz, and the HAPPEX and G0 experiments at Jefferson Lab, have focussed on the strange quark content of the nucleon. These are reviewed in Ref. 123, where it is shown that they can also provide significant constraints on C_{1u} and C_{1d} which complement those from atomic parity violation.

The parity violating asymmetry, A_{PV} , in fixed target polarized Møller scattering, $e^-e^- \rightarrow e^-e^-$, is defined as in Eq. (10.20) and reads [124],

$$\frac{A_{PV}}{Q^2} = -2C_{2e} \frac{G_F}{\sqrt{2}\pi\alpha} \frac{1-y}{1+y^4+(1-y)^4}, \quad (10.23)$$

where y is again the energy transfer. It has been measured at low $Q^2 = 0.026$ GeV² in the SLAC E158 experiment [125], with the result $A_{PV} = (-1.31 \pm 0.14(\text{stat.}) \pm 0.10(\text{syst.})) \times 10^{-7}$. Expressed in terms of the weak mixing angle in the $\overline{\text{MS}}$ scheme, this yields $\hat{s}^2(Q^2) = 0.2403 \pm 0.0013$, and established the scale dependence of the weak mixing (see Fig. 10.1) at the level of 6.4 standard deviations. One can also define the so-called weak charge of the electron (*cf.* Eq. (10.24) below) as $Q_W(e) \equiv -2C_{2e} = -0.0403 \pm 0.0053$ (the implications are discussed in Ref. 126). In a similar experiment and at about the same Q^2 , Qweak at Jefferson Lab [127] will be able to measure the weak charge of the proton, $Q_W(p) = -2[2C_{1u} + C_{1d}]$, and $\sin^2\theta_W$ in polarized ep scattering with relative precisions of 4% and 0.3%, respectively. These experiments will provide the most precise determinations of the weak mixing angle off the Z peak and will be sensitive to various types of physics beyond the SM.

There are precise experiments measuring atomic parity violation (APV) [131] in cesium [132,133] (at the 0.4% level [132]), thallium [134], lead [135], and bismuth [136]. The electroweak physics is contained in the weak charges which are defined by,

$$Q_W(Z, N) \equiv -2[C_{1u}(2Z + N) + C_{1d}(Z + 2N)] \approx Z(1 - 4\sin^2\theta_W) - N. \quad (10.24)$$

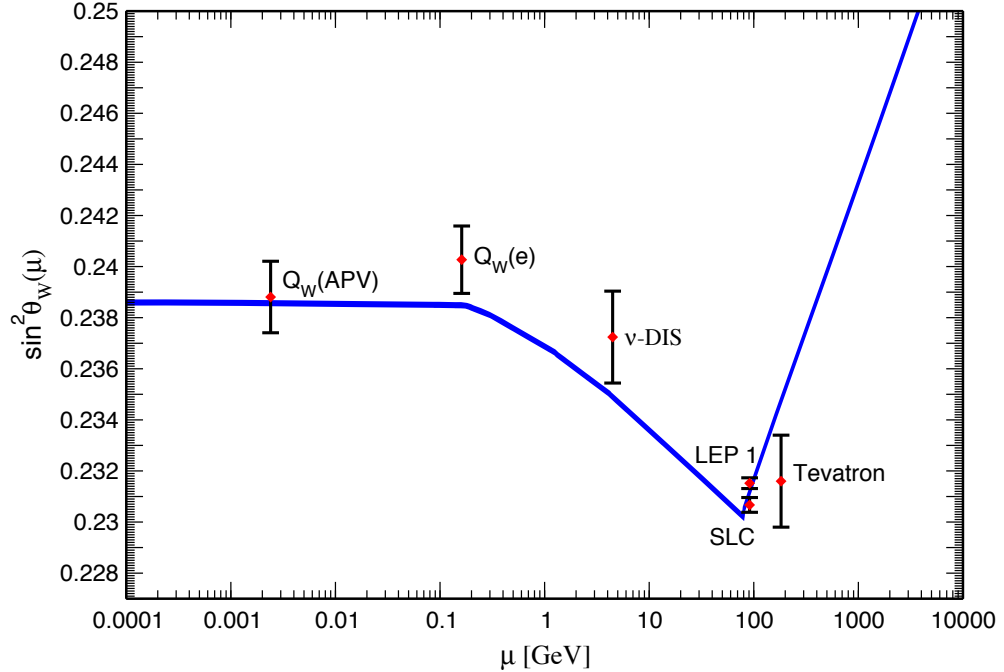


Figure 10.1: Scale dependence of the weak mixing angle defined in the $\overline{\text{MS}}$ scheme [129] (for the scale dependence of the weak mixing angle defined in a mass-dependent renormalization scheme, see Ref. 126). The minimum of the curve corresponds to $Q = M_W$, below which we switch to an effective theory with the W^\pm bosons integrated out, and where the β -function for the weak mixing angle changes sign. At the location of the W boson mass and each fermion mass, there are also discontinuities arising from scheme dependent matching terms which are necessary to ensure that the various effective field theories within a given loop order describe the same physics. However, in the $\overline{\text{MS}}$ scheme these are very small numerically and barely visible in the figure provided one decouples quarks at $Q = \hat{m}_q(\hat{m}_q)$. The width of the curve reflects the theory uncertainty from strong interaction effects which at low energies is at the level of $\pm 7 \times 10^{-5}$ [129]. Following the estimate [130] of the typical momentum transfer for parity violation experiments in Cs, the location of the APV data point is given by $\mu = 2.4$ MeV. For ν -DIS we chose $\mu = 20$ GeV which is about half-way between the averages of $\sqrt{Q^2}$ for ν and $\bar{\nu}$ interactions at NuTeV. The Tevatron measurements are strongly dominated by invariant masses of the final state dilepton pair of $\mathcal{O}(M_Z)$ and can thus be considered as additional Z pole data points, yielding $\bar{s}_Z^2 = 0.2316 \pm 0.0018$. However, for clarity we displayed the point horizontally to the right.

E.g., $Q_W(^{133}\text{Cs})$ is extracted by measuring experimentally the ratio of the parity violating amplitude, E_{PNC} , to the Stark vector transition polarizability, β , and by calculating theoretically E_{PNC} in terms of Q_W . One can then write,

$$Q_W = N \left(\frac{\text{Im } E_{\text{PNC}}}{\beta} \right)_{\text{exp.}} \left(\frac{|e| a_B}{\text{Im } E_{\text{PNC}}} \frac{Q_W}{N} \right)_{\text{th.}} \left(\frac{\beta}{a_B^3} \right)_{\text{exp.+th.}} \left(\frac{a_B^2}{|e|} \right).$$

16 10. Electroweak model and constraints on new physics

The uncertainties associated with atomic wave functions are quite small for cesium [137]. In the past, the semi-empirical value of β added another source of theoretical uncertainty [138]. The ratio of the off-diagonal hyperfine amplitude to the polarizability has now been measured directly by the Boulder group [139]. Combined with the precisely known hyperfine amplitude [140] one finds, $\beta = 26.991 \pm 0.046$, in excellent agreement with the earlier results, reducing the overall theory uncertainty (while slightly increasing the experimental error). The very recent state-of-the-art many body calculation [141] yields, $\text{Im } E_{\text{PNC}} = (0.8906 \pm 0.0026) \times 10^{-11} |e| a_B Q_W / N$, while the two measurements [132,133] combine to give $\text{Im } E_{\text{PNC}} / \beta = -1.5924 \pm 0.0055$ mV/cm, and we obtain $Q_W(^{133}_{78}\text{Cs}) = -73.20 \pm 0.35$. Thus, the various theoretical efforts in Refs. 141 and 142 together with an update of the SM calculation [128] removed an earlier 2.3σ deviation from the SM (see the year 2000 edition of this *Review*). The theoretical uncertainties are 3% for thallium [143] but larger for the other atoms. The Boulder experiment in cesium also observed the parity-violating weak corrections to the nuclear electromagnetic vertex (the anapole moment [144]).

In the future it could be possible to further reduce the theoretical wave function uncertainties by taking the ratios of parity violation in different isotopes [131,145]. There would still be some residual uncertainties from differences in the neutron charge radii, however [146]. Experiments in hydrogen and deuterium are another possibility for reducing the uncertainties [147].

10.4. W and Z boson physics

10.4.1. e^+e^- scattering below the Z pole :

The forward-backward asymmetry for $e^+e^- \rightarrow \ell^+\ell^-$, $\ell = \mu$ or τ , is defined as

$$A_{FB} \equiv \frac{\sigma_F - \sigma_B}{\sigma_F + \sigma_B}, \quad (10.25)$$

where $\sigma_F(\sigma_B)$ is the cross-section for ℓ^- to travel forward (backward) with respect to the e^- direction. A_{FB} and R , the total cross-section relative to pure QED, are given by

$$R = F_1, \quad A_{FB} = \frac{3}{4} \frac{F_2}{F_1}, \quad (10.26)$$

where

$$F_1 = 1 - 2\chi_0 g_V^e g_V^\ell \cos \delta_R + \chi_0^2 (g_V^{e2} + g_A^{e2}) (g_V^{\ell 2} + g_A^{\ell 2}), \quad (10.27a)$$

$$F_2 = -2\chi_0 g_A^e g_A^\ell \cos \delta_R + 4\chi_0^2 g_A^e g_A^\ell g_V^e g_V^\ell, \quad (10.27b)$$

$$\tan \delta_R = \frac{M_Z \Gamma_Z}{M_Z^2 - s}, \quad \chi_0 = \frac{G_F}{2\sqrt{2}\pi\alpha} \frac{s M_Z^2}{[(M_Z^2 - s)^2 + M_Z^2 \Gamma_Z^2]^{1/2}}, \quad (10.28)$$

and where \sqrt{s} is the CM energy. Eq. (10.27) is valid at tree level. If the data are radiatively corrected for QED effects (as described above), then the remaining electroweak

corrections can be incorporated [148,149] (in an approximation adequate for existing PEP, PETRA, and TRISTAN data, which are well below the Z pole) by replacing χ_0 by $\chi(s) \equiv (1 + \rho_t) \chi_0(s) \alpha/\alpha(s)$, where $\alpha(s)$ is the running QED coupling, and evaluating g_V in the $\overline{\text{MS}}$ scheme. Reviews and formulae for $e^+e^- \rightarrow \text{hadrons}$ may be found in Ref. 150.

10.4.2. Z pole physics :

At LEP 1 and SLC, there were high-precision measurements of various Z pole observables [11,151–156], as summarized in Table 10.7. These include the Z mass and total width, Γ_Z , and partial widths $\Gamma(f\bar{f})$ for $Z \rightarrow f\bar{f}$ where fermion $f = e, \mu, \tau$, hadrons, b , or c . It is convenient to use the variables $M_Z, \Gamma_Z, R_\ell \equiv \Gamma(\text{had})/\Gamma(\ell^+\ell^-)$ ($\ell = e, \mu, \tau$), $\sigma_{\text{had}} \equiv 12\pi \Gamma(e^+e^-) \Gamma(\text{had})/M_Z^2 \Gamma_Z^2$, $R_b \equiv \Gamma(b\bar{b})/\Gamma(\text{had})$, and $R_c \equiv \Gamma(c\bar{c})/\Gamma(\text{had})$, most of which are weakly correlated experimentally. ($\Gamma(\text{had})$ is the partial width into hadrons.) The three values for R_ℓ are not inconsistent with lepton universality (although R_τ is somewhat low), but we use the general analysis in which the three observables are treated as independent. Similar remarks apply to $A_{FB}^{0,\ell}$ below ($A_{FB}^{0,\tau}$ is somewhat high). $\mathcal{O}(\alpha^3)$ QED corrections introduce a large anti-correlation (-30%) between Γ_Z and σ_{had} . The anti-correlation between R_b and R_c is -18% [11]. The R_ℓ are insensitive to m_t except for the $Z \rightarrow b\bar{b}$ vertex and final state corrections and the implicit dependence through $\sin^2 \theta_W$. Thus, they are especially useful for constraining α_s . The width for invisible decays [11], $\Gamma(\text{inv}) = \Gamma_Z - 3\Gamma(\ell^+\ell^-) - \Gamma(\text{had}) = 499.0 \pm 1.5$ MeV, can be used to determine the number of neutrino flavors much lighter than $M_Z/2$, $N_\nu = \Gamma(\text{inv})/\Gamma^{\text{theory}}(\nu\bar{\nu}) = 2.984 \pm 0.009$ for $(m_t, M_H) = (173.1, 117)$ GeV.

There were also measurements of various Z pole asymmetries. These include the polarization or left-right asymmetry

$$A_{LR} \equiv \frac{\sigma_L - \sigma_R}{\sigma_L + \sigma_R}, \quad (10.29)$$

where $\sigma_L(\sigma_R)$ is the cross-section for a left-(right-)handed incident electron. A_{LR} was measured precisely by the SLD collaboration at the SLC [152], and has the advantages of being extremely sensitive to $\sin^2 \theta_W$ and that systematic uncertainties largely cancel. In addition, SLD extracted the final-state couplings (defined below), A_b, A_c [11], A_s [153], A_τ , and A_μ [154], from left-right forward-backward asymmetries, using

$$A_{LR}^{FB}(f) = \frac{\sigma_{LF}^f - \sigma_{LB}^f - \sigma_{RF}^f + \sigma_{RB}^f}{\sigma_{LF}^f + \sigma_{LB}^f + \sigma_{RF}^f + \sigma_{RB}^f} = \frac{3}{4} A_f, \quad (10.30)$$

where, for example, σ_{LF}^f is the cross-section for a left-handed incident electron to produce a fermion f traveling in the forward hemisphere. Similarly, A_τ was measured at LEP 1 [11] through the negative total τ polarization, \mathcal{P}_τ , and A_e was extracted from the angular distribution of \mathcal{P}_τ . An equation such as (10.30) assumes that initial state QED corrections, photon exchange, γ - Z interference, the tiny electroweak boxes, and corrections for $\sqrt{s} \neq M_Z$ are removed from the data, leaving the pure electroweak asymmetries. This allows the use of effective tree-level expressions,

$$A_{LR} = A_e P_e, \quad A_{FB} = \frac{3}{4} A_f \frac{A_e + P_e}{1 + P_e A_e}, \quad (10.31)$$

18 10. Electroweak model and constraints on new physics

where

$$A_f \equiv \frac{2\bar{g}_V^f \bar{g}_A^f}{\bar{g}_V^{f2} + \bar{g}_A^{f2}}, \quad (10.32)$$

and

$$\bar{g}_V^f = \sqrt{\rho_f} (t_{3L}^{(f)} - 2q_f \kappa_f \sin^2 \theta_W), \quad \bar{g}_A^f = \sqrt{\rho_f} t_{3L}^{(f)}. \quad (10.33)$$

P_e is the initial e^- polarization, so that the second equality in Eq. (10.30) is reproduced for $P_e = 1$, and the Z pole forward-backward asymmetries at LEP 1 ($P_e = 0$) are given by $A_{FB}^{(0,f)} = \frac{3}{4} A_e A_f$ where $f = e, \mu, \tau, b, c, s$ [155], and q , and where $A_{FB}^{(0,q)}$ refers to the hadronic charge asymmetry. Corrections for t -channel exchange and s/t -channel interference cause $A_{FB}^{(0,e)}$ to be strongly anti-correlated with R_e (-37%). The correlation between $A_{FB}^{(0,b)}$ and $A_{FB}^{(0,c)}$ amounts to 15%. The initial state coupling, A_e , was also determined through the left-right charge asymmetry [156] and in polarized Bhabba scattering [154] at the SLC. The forward-backward asymmetry, A_{FB} , for e^+e^- final states (with invariant masses restricted to or dominated by values around M_Z) in $p\bar{p}$ collisions has been measured by the CDF [157] and DØ [158] collaborations and values for \bar{s}_ℓ^2 were extracted, which combine to $\bar{s}_\ell^2 = 0.2316 \pm 0.0018$. By varying the invariant mass and the scattering angle (and assuming the electron couplings), the effective Z couplings to light quarks, $\bar{g}_{V,A}^{u,d}$, resulted, as well, but with large uncertainties and mutual correlations and not independently of \bar{s}_ℓ^2 above. Similar analyses have also been reported by the H1 and ZEUS collaborations at HERA [159] and by the LEP collaborations [11].

The electroweak radiative corrections have been absorbed into corrections $\rho_f - 1$ and $\kappa_f - 1$, which depend on the fermion f and on the renormalization scheme. In the on-shell scheme, the quadratic m_t dependence is given by $\rho_f \sim 1 + \rho_t$, $\kappa_f \sim 1 + \rho_t / \tan^2 \theta_W$, while in $\overline{\text{MS}}$, $\hat{\rho}_f \sim \hat{\kappa}_f \sim 1$, for $f \neq b$ ($\hat{\rho}_b \sim 1 - \frac{4}{3}\rho_t$, $\hat{\kappa}_b \sim 1 + \frac{2}{3}\rho_t$). In the $\overline{\text{MS}}$ scheme the normalization is changed according to $G_F M_Z^2 / 2\sqrt{2}\pi \rightarrow \hat{\alpha} / 4\hat{s}_Z^2 \hat{c}_Z^2$. (If one continues to normalize amplitudes by $G_F M_Z^2 / 2\sqrt{2}\pi$, as in the 1996 edition of this *Review*, then $\hat{\rho}_f$ contains an additional factor of $\hat{\rho}$.) In practice, additional bosonic and fermionic loops, vertex corrections, leading higher order contributions, *etc.*, must be included. For example, in the $\overline{\text{MS}}$ scheme one has $\hat{\rho}_\ell = 0.9981$, $\hat{\kappa}_\ell = 1.0013$, $\hat{\rho}_b = 0.9870$, and $\hat{\kappa}_b = 1.0067$. It is convenient to define an effective angle $\bar{s}_f^2 \equiv \sin^2 \bar{\theta}_{Wf} \equiv \hat{\kappa}_f \hat{s}_Z^2 = \kappa_f s_W^2$, in terms of which \bar{g}_V^f and \bar{g}_A^f are given by $\sqrt{\rho_f}$ times their tree-level formulae. Because \bar{g}_V^ℓ is very small, not only $A_{LR}^0 = A_e$, $A_{FB}^{(0,\ell)}$, and \mathcal{P}_τ , but also $A_{FB}^{(0,b)}$, $A_{FB}^{(0,c)}$, $A_{FB}^{(0,s)}$, and the hadronic asymmetries are mainly sensitive to \bar{s}_ℓ^2 . One finds that $\hat{\kappa}_f$ ($f \neq b$) is almost independent of (m_t, M_H) , so that one can write

$$\bar{s}_\ell^2 \sim \hat{s}_Z^2 + 0.00029. \quad (10.34)$$

Thus, the asymmetries determine values of \bar{s}_ℓ^2 and \hat{s}_Z^2 almost independent of m_t , while the κ 's for the other schemes are m_t dependent.

10.4.3. LEP 2 :

LEP 2 [160] ran at several energies above the Z pole up to ~ 209 GeV. Measurements were made of a number of observables, including the cross-sections for $e^+e^- \rightarrow f\bar{f}$ for $f = q, \mu^-, \tau^-$; the differential cross-sections for $f = e^-, \mu^-, \tau^-$; R_q for $q = b, c$; $A_{FB}(f)$ for $f = \mu, \tau, b, c$; W branching ratios; and WW , $WW\gamma$, ZZ , single W , and single Z cross-sections. They are in good agreement with the SM predictions, with the exceptions of the total hadronic cross-section (1.7σ high), R_b (2.1σ low), and $A_{FB}(b)$ (1.6σ low). Also, the negative result of the direct search for the SM Higgs boson excluded M_H values below 114.4 GeV at the 95% CL [161]. This result is complementary to and can be combined with [162] the limits inferred from the electroweak precision data.

The Z boson properties are extracted assuming the SM expressions for the γ - Z interference terms. These have also been tested experimentally by performing more general fits [160,163] to the LEP 1 and LEP 2 data. Assuming family universality this approach introduces three additional parameters relative to the standard fit [11], describing the γ - Z interference contribution to the total hadronic and leptonic cross-sections, $j_{\text{had}}^{\text{tot}}$ and j_ℓ^{tot} , and to the leptonic forward-backward asymmetry, j_ℓ^{fb} . *E.g.*,

$$j_{\text{had}}^{\text{tot}} \sim g_V^\ell g_V^{\text{had}} = 0.277 \pm 0.065, \quad (10.35)$$

which is in agreement with the SM expectation [11] of 0.21 ± 0.01 . These are valuable tests of the SM; but it should be cautioned that new physics is not expected to be described by this set of parameters, since (i) they do not account for extra interactions beyond the standard weak neutral-current, and (ii) the photonic amplitude remains fixed to its SM value.

Strong constraints on anomalous triple and quartic gauge couplings have been obtained at LEP 2 and the Tevatron as described in the Gauge & Higgs Bosons Particle Listings.

10.4.4. W and Z decays :

The partial decay width for gauge bosons to decay into massless fermions $f_1\bar{f}_2$ (the numerical values include the small electroweak radiative corrections and final state mass effects) is

$$\Gamma(W^+ \rightarrow e^+\nu_e) = \frac{G_F M_W^3}{6\sqrt{2}\pi} \approx 226.31 \pm 0.07 \text{ MeV}, \quad (10.36a)$$

$$\Gamma(W^+ \rightarrow u_i\bar{d}_j) = \frac{CG_F M_W^3}{6\sqrt{2}\pi} |V_{ij}|^2 \approx 706.18 \pm 0.22 \text{ MeV} |V_{ij}|^2, \quad (10.36b)$$

$$\Gamma(Z \rightarrow \psi_i\bar{\psi}_i) = \frac{CG_F M_Z^3}{6\sqrt{2}\pi} [g_V^{i2} + g_A^{i2}]$$

$$\approx \begin{cases} 167.21 \pm 0.02 \text{ MeV} (\nu\bar{\nu}), \\ 83.99 \pm 0.01 \text{ MeV} (e^+e^-), \\ 300.20 \pm 0.06 \text{ MeV} (u\bar{u}), \\ 382.98 \pm 0.06 \text{ MeV} (d\bar{d}), \\ 375.94 \mp 0.04 \text{ MeV} (b\bar{b}). \end{cases} \quad (10.36c)$$

20 10. Electroweak model and constraints on new physics

For leptons $C = 1$, while for quarks

$$C = 3 \left[1 + \frac{\alpha_s(M_V)}{\pi} + 1.409 \frac{\alpha_s^2}{\pi^2} - 12.77 \frac{\alpha_s^3}{\pi^3} - 80.0 \frac{\alpha_s^4}{\pi^4} \right], \quad (10.37)$$

where the 3 is due to color and the factor in brackets represents the universal part of the QCD corrections [164] for massless quarks [165]. The $\mathcal{O}(\alpha_s^4)$ contribution in Eq. (10.37) is new [166]. The $Z \rightarrow f\bar{f}$ widths contain a number of additional corrections: universal (non-singlet) top quark mass contributions [167]; fermion mass effects and further QCD corrections proportional to $\hat{m}_q^2(M_Z^2)$ [168] which are different for vector and axial-vector partial widths; and singlet contributions starting from two-loop order which are large, strongly top quark mass dependent, family universal, and flavor non-universal [169]. The QED factor $1 + 3\alpha q_f^2/4\pi$, as well as two-loop order $\alpha\alpha_s$ and α^2 self-energy corrections [170] are also included. Working in the on-shell scheme, *i.e.*, expressing the widths in terms of $G_F M_{W,Z}^3$, incorporates the largest radiative corrections from the running QED coupling [61,171]. Electroweak corrections to the Z widths are then incorporated by replacing $g_{V,A}^2$ by $\bar{g}_{V,A}^2$. Hence, in the on-shell scheme the Z widths are proportional to $\rho_i \sim 1 + \rho_t$. The $\overline{\text{MS}}$ normalization accounts also for the leading electroweak corrections [66]. There is additional (negative) quadratic m_t dependence in the $Z \rightarrow b\bar{b}$ vertex corrections [172] which causes $\Gamma(b\bar{b})$ to decrease with m_t . The dominant effect is to multiply $\Gamma(b\bar{b})$ by the vertex correction $1 + \delta\rho_{b\bar{b}}$, where $\delta\rho_{b\bar{b}} \sim 10^{-2}(-\frac{1}{2}\frac{m_t^2}{M_Z^2} + \frac{1}{5})$. In practice, the corrections are included in ρ_b and κ_b , as discussed before.

For 3 fermion families the total widths are predicted to be

$$\Gamma_Z \approx 2.4957 \pm 0.0003 \text{ GeV} , \quad \Gamma_W \approx 2.0910 \pm 0.0007 \text{ GeV} . \quad (10.38)$$

We have assumed $\alpha_s(M_Z) = 0.1200$. An uncertainty in α_s of ± 0.0016 introduces an additional uncertainty of 0.05% in the hadronic widths, corresponding to ± 0.8 MeV in Γ_Z . These predictions are to be compared with the experimental results $\Gamma_Z = 2.4952 \pm 0.0023$ GeV [11] and $\Gamma_W = 2.085 \pm 0.042$ GeV [173] (see the Gauge & Higgs Boson Particle Listings for more details).

10.5. Precision flavor physics

In addition to cross-sections, asymmetries, parity violation, W and Z decays, there is a large number of experiments and observables testing the flavor structure of the SM. These are addressed elsewhere in this *Review*, and generally not included in this Section. However, we identify three precision observables with sensitivity to similar types of new physics as the other processes discussed here. The branching fraction of the flavor changing transition $b \rightarrow s\gamma$ is of comparatively low precision, but since it is a loop-level process (in the SM) its sensitivity to new physics (and SM parameters, such as heavy quark masses) is enhanced. The τ -lepton lifetime and leptonic branching

ratios are primarily sensitive to α_s and not affected significantly by many types of new physics. However, having an independent and reliable low energy measurement of α_s in a global analysis allows the comparison with the Z lineshape determination of α_s which shifts easily in the presence of new physics contributions. By far the most precise observable discussed here is the anomalous magnetic moment of the muon (the electron magnetic moment is measured to even greater precision, but its new physics sensitivity is suppressed by an additional factor of m_e^2/m_μ^2). Its combined experimental and theoretical uncertainty is comparable to typical new physics contributions.

The CLEO [174], BaBar [175] and Belle [176] collaborations reported precise measurements of the process $b \rightarrow s\gamma$. We extrapolated these results to the full photon spectrum which is defined according to the recommendation in Ref. 177. The results for the branching fractions are then given by,

$$\begin{aligned} \text{CLEO} &: 3.32 \times 10^{-4} [1 \pm 0.134 \pm 0.076 \pm 0.038 \pm 0.048 \pm 0.003], \\ \text{BaBar(incl.)} &: 3.99 \times 10^{-4} [1 \pm 0.080 \pm 0.091 \pm 0.079 \pm 0.026 \pm 0.003], \\ \text{BaBar(excl.)} &: 3.57 \times 10^{-4} [1 \pm 0.055^{+0.168}_{-0.122} \pm 0 \pm 0.026 \pm 0], \\ \text{Belle} &: 3.61 \times 10^{-4} [1 \pm 0.043 \pm 0.116 \pm 0.003 \pm 0.014 \pm 0.003], \end{aligned}$$

where the first two errors are the statistical and systematic uncertainties (taken uncorrelated). In the cases of CLEO and Belle, the error component from the signal models are moved from the systematic error to the model (third) error. The fourth error accounts for the extrapolation from the finite photon energy cutoff [177–179] (2.0 GeV, 1.9 GeV, and 1.7 GeV, respectively, for CLEO, BaBar and Belle) to the full theoretical branching ratio. For this we use the results of Ref. 177 for $m_b = 4.70$ GeV which is in good agreement with the more recent Ref. 179. The uncertainty reflects the difference due to choosing $m_b = 4.60$ GeV, instead. The last error is from the correction (0.957 ± 0.003) for the $b \rightarrow d\gamma$ component which is common to all inclusive measurements, but absent for the exclusive BaBar measurement in the third line. The last three errors are taken as 100% correlated, resulting in the correlation matrix in Table 10.4. It is advantageous [180] to normalize the result with respect to the semi-leptonic branching fraction, $\mathcal{B}(b \rightarrow X e \nu) = 0.1074 \pm 0.0016$, yielding,

$$R = \frac{\mathcal{B}(b \rightarrow s\gamma)}{\mathcal{B}(b \rightarrow X e \nu)} = (3.38 \pm 0.27 \pm 0.37) \times 10^{-3}. \quad (10.39)$$

In the fits we use the variable $\ln R = -5.69 \pm 0.14$ to assure an approximately Gaussian error [181]. The second uncertainty in Eq. (10.39) is an 11% theory uncertainty (excluding parametric errors such as from α_s) in the SM prediction which is based on the next-to-leading order calculations of Refs. 180 and 182. There is a coordinated effort underway to obtain the SM prediction at next-to-next-to-leading order [183].

The extraction of α_s from the τ lifetime is standing out from other determinations because of a variety of independent reasons: (i) the τ -scale is low, so that upon extrapolation to the Z scale (where it can be compared to the theoretically clean

Table 10.4: Correlation matrix for measurements of $b \rightarrow s\gamma$.

CLEO	1.000	0.175	0.048	0.038
BaBar (inclusive)	0.175	1.000	0.029	0.033
BaBar (exclusive)	0.048	0.029	1.000	0.019
Belle	0.038	0.033	0.019	1.000

Z lineshape determinations) the α_s error shrinks by about an order of magnitude; (ii) yet, this scale is high enough that perturbation theory and the operator product expansion (OPE) can be applied; (iii) these observables are fully inclusive and thus free of fragmentation and hadronization effects that would have to be modeled or measured; (iv) OPE breaking effects are most problematic near the branch cut but there they are suppressed by a double zero at $s = m_\tau^2$; (v) there are enough data [41,43] to constrain non-perturbative effects both within and breaking the OPE; (vi) a complete four-loop order QCD calculation is available [166]; (vii) large effects associated with the QCD β -function can be re-summed [184] in what has become known as contour improved perturbation theory (CIPT). However, while there is no doubt that CIPT shows faster convergence in the lower (calculable) orders, doubts have been cast on the method by the observation that at least in a specific model [185], which includes the exactly known coefficients and theoretical constraints on the large-order behavior, ordinary fixed order perturbation theory (FOPT) may nevertheless give a better approximation to the full result. We therefore use the expressions [5,165,166,186],

$$\tau_\tau = \hbar \frac{1 - \mathcal{B}_\tau^s}{\Gamma_\tau^e + \Gamma_\tau^\mu + \Gamma_\tau^{ud}} = 291.09 \pm 0.48 \text{ fs}, \quad (10.40)$$

$$\begin{aligned} \Gamma_\tau^{ud} = & \frac{G_F^2 m_\tau^5 |V_{ud}|^2}{64\pi^3} S(m_\tau, M_Z) \left(1 + \frac{3}{5} \frac{m_\tau^2}{M_W^2} \right) \times \\ & \left[1 + \frac{\alpha_s(m_\tau)}{\pi} + 5.202 \frac{\alpha_s^2}{\pi^2} + 26.37 \frac{\alpha_s^3}{\pi^3} \right. \\ & \left. + 127.1 \frac{\alpha_s^4}{\pi^4} + \frac{\hat{\alpha}}{\pi} \left(\frac{85}{24} - \frac{\pi^2}{2} \right) \right], \quad (10.41) \end{aligned}$$

and Γ_τ^e and Γ_τ^μ can be taken from Eq. (10.4) with obvious replacements. The relative fraction of decays with $\Delta S = -1$, $\mathcal{B}_\tau^s = 0.0286 \pm 0.0007$, is based on experimental data since the value for the strange quark mass, $\hat{m}_s(m_\tau)$, is not well known and the QCD expansion proportional to \hat{m}_s^2 converges poorly and cannot be trusted. $S(m_\tau, M_Z) = 1.01907 \pm 0.0003$ is a logarithmically enhanced electroweak correction factor with higher orders re-summed [187]. Also included (but not shown) are quark

mass effects and condensate contributions [188]. The largest uncertainty arises from the truncation of the FOPT series and is conservatively taken as the α_s^4 term (this is re-calculated in each call of the fits, leading to an α_s -dependent and thus asymmetric error) until a better understanding of the numerical differences between FOPT and CIPT has been gained. Incidentally, the τ spectral functions are better described in CIPT than in FOPT [188]. Our error almost covers the entire range from using CIPT to assuming that the nearly geometric series in Eq. (10.41) continues to higher orders. The next largest uncertainties (± 0.6 fs) are from the condensates [188] and the evolution to the Z scale, followed by the experimental uncertainty in Eq. (10.40), which is from combining the two leptonic branching ratios with the direct τ_τ . Included are also various smaller uncertainties from other sources. In total we obtain a $\sim 1.5\%$ determination of $\alpha_s(M_Z) = 0.1174_{-0.0016}^{+0.0018}$ which updates the result of Ref. 5. For more details, see Refs. 50 and 188 where the τ spectral functions are used as additional input.

The world average of the muon anomalous magnetic moment**,

$$a_\mu^{\text{exp}} = \frac{g_\mu - 2}{2} = (1165920.80 \pm 0.63) \times 10^{-9}, \quad (10.42)$$

is dominated by the final result of the E821 collaboration at BNL [189]. The QED contribution has been calculated to four loops [190] (fully analytically to three loops [191,192]), and the leading logarithms are included to five loops [193,194]. The estimated SM electroweak contribution [195–197], $a_\mu^{\text{EW}} = (1.52 \pm 0.03) \times 10^{-9}$, which includes leading two-loop [196] and three-loop [197] corrections, is at the level of twice the current uncertainty.

The limiting factor in the interpretation of the result is the uncertainty from the two-loop hadronic contribution. *E.g.*, Ref. 50 obtained the value $a_\mu^{\text{had}} = (69.55 \pm 0.41) \times 10^{-9}$ which combines CMD-2 [45] and SND [46] $e^+e^- \rightarrow$ hadrons cross-section data with radiative return results from BaBar [48] and KLOE [49]. This value suggests a 3.1σ discrepancy between Eq. (10.42) and the SM prediction. Updating an alternative analysis [39] the authors of Ref. 40 quote $a_\mu^{\text{had}} = (70.53 \pm 0.45) \times 10^{-9}$ using τ decay data and isospin symmetry (CVC). This result implies a smaller conflict (1.8σ) with Eq. (10.42). Thus, there is also a discrepancy between the 2π and 4π spectral functions obtained from the two methods, contributing 70% and 30% of the discrepancy, respectively. For example, if one uses the e^+e^- data and CVC to predict the branching ratio for $\tau^- \rightarrow \nu_\tau \pi^- \pi^0$ decays one obtains $24.78 \pm 0.25\%$ [40], while the average of

** In what follows, we summarize the most important aspects of $g_\mu - 2$, and give some details about the evaluation in our fits. For more details see the dedicated contribution by A. Höcker and W. Marciano in this *Review*. There are some small numerical differences (at the level of 0.1 standard deviation), which are well understood and mostly arise because internal consistency of the fits requires the calculation of all observables from analytical expressions and common inputs and fit parameters, so that an independent evaluation is necessary for this Section. Note, that in the spirit of a global analysis based on all available information we have chosen here to average in the τ decay and radiative return (KLOE and BaBar) data, as well.

24 10. Electroweak model and constraints on new physics

the directly measured branching ratio yields $25.51 \pm 0.09\%$ which is 2.7σ higher. It is important to understand the origin of this difference, but two observations point to the conclusion that at least some of it is experimental: (i) The $\tau^- \rightarrow \nu_\tau 2\pi^- \pi^+ \pi^0$ spectral function also disagrees with the corresponding e^+e^- data by 1.7σ , which translates to a 20% effect [40,50] and seems too large to arise from isospin violation. (ii) Isospin violating corrections have been studied in detail in Refs. 40 and 198 and found to be largely under control. The largest effect is due to higher-order electroweak corrections [52] but introduces a negligible uncertainty [187]. Nevertheless, a_μ^{had} is often evaluated excluding the τ decay data arguing [199] that CVC breaking effects (*e.g.*, through a relatively large mass difference between the ρ^\pm and ρ^0 vector mesons) may be larger than expected. (This may also be relevant [199] in the context of the NuTeV result discussed above.) Experimentally [43], this mass difference is indeed larger than expected, but then one would also expect a significant width difference which is contrary to observation [43]. Fortunately, due to the suppression at large s (from where the conflicts originate) these problems are less pronounced as far as a_μ^{had} is concerned. In the following we view all differences in spectral functions as (systematic) fluctuations and average the results.

Table 10.5: Principal SM fit result including mutual correlations (all masses in GeV).

M_Z	91.1874 ± 0.0021	1.00	-0.01	0.00	0.00	-0.01	0.00	0.12
$\hat{m}_t(\hat{m}_t)$	163.5 ± 1.3	-0.01	1.00	0.00	0.00	-0.10	0.00	0.39
$\hat{m}_b(\hat{m}_b)$	4.198 ± 0.023	0.00	0.00	1.00	0.25	-0.04	0.01	0.04
$\hat{m}_c(\hat{m}_c)$	$1.266^{+0.031}_{-0.036}$	0.00	0.00	0.25	1.00	0.08	0.02	0.12
$\alpha_s(M_Z)$	0.1183 ± 0.0015	-0.01	-0.10	-0.04	0.08	1.00	0.00	-0.04
$\Delta\alpha_{\text{had}}^{(3)}(1.8 \text{ GeV})$	0.00574 ± 0.00010	0.00	-0.01	0.01	0.02	0.00	1.00	-0.18
M_H	90^{+27}_{-22}	0.12	0.39	0.04	0.12	-0.04	-0.18	1.00

An additional uncertainty is induced by the hadronic three-loop light-by-light scattering contribution. Two recent and inherently different model calculations yield $a_\mu^{\text{LBLS}} = (+1.36 \pm 0.25) \times 10^{-9}$ [200] and $a_\mu^{\text{LBLS}} = +1.37^{+0.15}_{-0.27} \times 10^{-9}$ [201] which are higher than previous evaluations [202,203]. The sign of this effect is opposite [202] to the one quoted in the 2002 edition of this *Review*, and has subsequently been confirmed by two other groups [203]. There is also the upper bound $a_\mu^{\text{LBLS}} < 1.59 \times 10^{-9}$ [201] but this requires an ad hoc assumption, too. The very recent Ref. 204 quotes the value $a_\mu^{\text{LBLS}} = (+1.05 \pm 0.26) \times 10^{-9}$, which we shift by 2×10^{-11} to account for the more accurate charm quark treatment of Ref. 201. We also increase the error to cover all evaluations, and we will use $a_\mu^{\text{LBLS}} = (+1.07 \pm 0.32) \times 10^{-9}$ in the fits.

Other hadronic effects at three-loop order contribute [205] $a_\mu^{\text{had}}(\alpha^3) = (-1.00 \pm$

$0.06) \times 10^{-9}$. Correlations with the two-loop hadronic contribution and with $\Delta\alpha(M_Z)$ (see Sec. 10.2) were considered in Ref. 192 which also contains analytic results for the perturbative QCD contribution.

Altogether, the SM prediction is

$$a_\mu^{\text{theory}} = (1165918.90 \pm 0.44) \times 10^{-9} , \quad (10.43)$$

where the error is from the hadronic uncertainties excluding parametric ones such as from α_s and the heavy quark masses. We estimate its correlation with $\Delta\alpha(M_Z)$ to 14%. The overall 2.5σ discrepancy between the experimental and theoretical values could be due to fluctuations (the E821 result is statistics dominated) or underestimates of the theoretical uncertainties. On the other hand, $g_\mu - 2$ is also affected by many types of new physics, such as supersymmetric models with large $\tan\beta$ and moderately light superparticle masses [206]. Thus, the deviation could also arise from physics beyond the SM.

10.6. Experimental results

The values for m_t [6], M_W [160,207], neutrino scattering [98,114–116], the weak charges of the electron [125], cesium [132,133] and thallium [134], the $b \rightarrow s\gamma$ observable [174–175], the muon anomalous magnetic moment [189], and the τ lifetime are listed in Table 10.6. Likewise, the principal Z pole observables can be found in Table 10.7 where the LEP 1 averages of the ALEPH, DELPHI, L3, and OPAL results include common systematic errors and correlations [11]. The heavy flavor results of LEP 1 and SLD are based on common inputs and correlated, as well [11]. Note that the values of $\Gamma(\ell^+\ell^-)$, $\Gamma(\text{had})$, and $\Gamma(\text{inv})$ are not independent of Γ_Z , the R_ℓ , and σ_{had} and that the SM errors in those latter are largely dominated by the uncertainty in α_s . Also shown in both Tables are the SM predictions for the values of M_Z , M_H , $\alpha_s(M_Z)$, $\Delta\alpha_{\text{had}}^{(3)}$ and the heavy quark masses shown in Table 10.5. The predictions result from a global least-square (χ^2) fit to all data using the minimization package MINUIT [208] and the electroweak library GAPP [90]. In most cases, we treat all input errors (the uncertainties of the values) as Gaussian. The reason is not that we assume that theoretical and systematic errors are intrinsically bell-shaped (which they are not) but because in most cases the input errors are combinations of many different (including statistical) error sources, which should yield approximately Gaussian *combined* errors by the large number theorem. Thus, it suffices if either the statistical components dominate or there are many components of similar size. An exception is the theory dominated error on the τ lifetime, which we recalculate in each χ^2 -function call since it depends itself on α_s . Sizes and shapes of the output errors (the uncertainties of the predictions and the SM fit parameters) are fully determined by the fit, and 1σ errors are defined to correspond to $\Delta\chi^2 = \chi^2 - \chi_{\text{min}}^2 = 1$, and do not necessarily correspond to the 68.3% probability range or the 39.3% probability contour (for 2 parameters).

The agreement is generally very good. Despite the few discrepancies discussed in the following, the fit describes well the data with a $\chi^2/\text{d.o.f.} = 43.0/44$. Only the final result for $g_\mu - 2$ from BNL and $A_{FB}^{(0,b)}$ from LEP 1 are currently showing large (2.5σ and 2.7σ)

Table 10.6: Principal non- Z pole observables, compared with the SM best fit predictions. The first M_W value is from the Tevatron [207] and the second one from LEP 2 [160]. The values of M_W and m_t differ from those in the Particle Listings when they include recent preliminary results. g_L^2 , which has been adjusted as discussed in Sec. 10.3, and g_R^2 are from NuTeV [98] and have a very small (-1.7%) residual anti-correlation. e -DIS [123] and the older ν -DIS constraints from CDHS [92], CHARM [93], and CCFR [94] are included, as well, but not shown in the Table. The world averages for $g_{V,A}^{\nu e}$ are dominated by the CHARM II [116] results, $g_V^{\nu e} = -0.035 \pm 0.017$ and $g_A^{\nu e} = -0.503 \pm 0.017$. The errors are the total (experimental plus theoretical) uncertainties. The τ_τ value is the τ lifetime world average computed by combining the direct measurements with values derived from the leptonic branching ratios [5]; in this case, the theory uncertainty is included in the SM prediction. In all other SM predictions, the uncertainty is from M_Z , M_H , m_t , m_b , m_c , $\hat{\alpha}(M_Z)$, and α_s , and their correlations have been accounted for. The column denoted Pull gives the standard deviations for the principal fit with M_H free, while the column denoted Dev. (Deviation) is for $M_H = 117$ GeV fixed.

Quantity	Value	Standard Model	Pull	Dev.
m_t [GeV]	173.1 ± 1.3	173.2 ± 1.3	-0.1	-0.5
M_W [GeV]	80.420 ± 0.031	80.384 ± 0.014	1.2	1.5
	80.376 ± 0.033		-0.2	0.1
g_L^2	0.3027 ± 0.0018	0.30399 ± 0.00017	-0.7	-0.6
g_R^2	0.0308 ± 0.0011	0.03001 ± 0.00002	0.7	0.7
$g_V^{\nu e}$	-0.040 ± 0.015	-0.0398 ± 0.0003	0.0	0.0
$g_A^{\nu e}$	-0.507 ± 0.014	-0.5064 ± 0.0001	0.0	0.0
$Q_W(e)$	-0.0403 ± 0.0053	-0.0473 ± 0.0005	1.3	1.2
$Q_W(\text{Cs})$	-73.20 ± 0.35	-73.15 ± 0.02	-0.1	-0.1
$Q_W(\text{Tl})$	-116.4 ± 3.6	-116.76 ± 0.04	0.1	0.1
τ_τ [fs]	291.09 ± 0.48	290.02 ± 2.09	0.5	0.5
$\frac{\Gamma(b \rightarrow s\gamma)}{\Gamma(b \rightarrow X e \nu)}$	$(3.38^{+0.51}_{-0.44}) \times 10^{-3}$	$(3.11 \pm 0.07) \times 10^{-3}$	0.6	0.6
$\frac{1}{2}(g_\mu - 2 - \frac{\alpha}{\pi})$	$(4511.07 \pm 0.77) \times 10^{-9}$	$(4509.13 \pm 0.08) \times 10^{-9}$	2.5	2.5

deviations. In addition, A_{LR}^0 (SLD) from hadronic final states differs by 1.8σ . The SM prediction of σ_{had} (LEP 1) moved closer to the measurement value which is slightly higher. R_b , whose measured value deviated in the past by as much as 3.7σ from the SM prediction, is now in agreement, and a 2σ discrepancy in $Q_W(\text{Cs})$ has also been resolved. g_L^2 from NuTeV is currently in agreement with the SM but this statement is preliminary (see Sec. 10.3).

A_b can be extracted from $A_{FB}^{(0,b)}$ when $A_e = 0.1501 \pm 0.0016$ is taken from a fit to

Table 10.7: Principal Z pole observables and their SM predictions (*cf.* Table 10.6). The first $\bar{s}_\ell^2(A_{FB}^{(0,q)})$ is the effective angle extracted from the hadronic charge asymmetry while the second is the combined lepton asymmetry from CDF [157] and DØ [158]. The three values of A_e are (i) from A_{LR} for hadronic final states [152]; (ii) from A_{LR} for leptonic final states and from polarized Bhabba scattering [154]; and (iii) from the angular distribution of the τ polarization at LEP 1. The two A_τ values are from SLD and the total τ polarization, respectively.

Quantity	Value	Standard Model	Pull	Dev.
M_Z [GeV]	91.1876 ± 0.0021	91.1874 ± 0.0021	0.1	0.0
Γ_Z [GeV]	2.4952 ± 0.0023	2.4954 ± 0.0009	-0.1	0.1
$\Gamma(\text{had})$ [GeV]	1.7444 ± 0.0020	1.7418 ± 0.0009	—	—
$\Gamma(\text{inv})$ [MeV]	499.0 ± 1.5	501.69 ± 0.07	—	—
$\Gamma(\ell^+\ell^-)$ [MeV]	83.984 ± 0.086	84.005 ± 0.015	—	—
σ_{had} [nb]	41.541 ± 0.037	41.484 ± 0.008	1.5	1.5
R_e	20.804 ± 0.050	20.735 ± 0.010	1.4	1.4
R_μ	20.785 ± 0.033	20.735 ± 0.010	1.5	1.6
R_τ	20.764 ± 0.045	20.780 ± 0.010	-0.4	-0.3
R_b	0.21629 ± 0.00066	0.21578 ± 0.00005	0.8	0.8
R_c	0.1721 ± 0.0030	0.17224 ± 0.00003	0.0	0.0
$A_{FB}^{(0,e)}$	0.0145 ± 0.0025	0.01633 ± 0.00021	-0.7	-0.7
$A_{FB}^{(0,\mu)}$	0.0169 ± 0.0013		0.4	0.6
$A_{FB}^{(0,\tau)}$	0.0188 ± 0.0017		1.5	1.6
$A_{FB}^{(0,b)}$	0.0992 ± 0.0016	0.1034 ± 0.0007	-2.7	-2.3
$A_{FB}^{(0,c)}$	0.0707 ± 0.0035	0.0739 ± 0.0005	-0.9	-0.8
$A_{FB}^{(0,s)}$	0.0976 ± 0.0114	0.1035 ± 0.0007	-0.6	-0.4
$\bar{s}_\ell^2(A_{FB}^{(0,q)})$	0.2324 ± 0.0012	0.23146 ± 0.00012	0.8	0.7
	0.2316 ± 0.0018		0.1	0.0
A_e	0.15138 ± 0.00216	0.1475 ± 0.0010	1.8	2.2
	0.1544 ± 0.0060		1.1	1.3
	0.1498 ± 0.0049		0.5	0.6
A_μ	0.142 ± 0.015		-0.4	-0.3
A_τ	0.136 ± 0.015		-0.8	-0.7
	0.1439 ± 0.0043		-0.8	-0.7
A_b	0.923 ± 0.020	0.9348 ± 0.0001	-0.6	-0.6
A_c	0.670 ± 0.027	0.6680 ± 0.0004	0.1	0.1
A_s	0.895 ± 0.091	0.9357 ± 0.0001	-0.4	-0.4

28 10. Electroweak model and constraints on new physics

leptonic asymmetries (using lepton universality). The result, $A_b = 0.881 \pm 0.017$, is 3.2σ below the SM prediction[†] and also 1.6σ below $A_b = 0.923 \pm 0.020$ obtained from $A_{LR}^{FB}(b)$ at SLD. Thus, it appears that at least some of the problem in $A_{FB}^{(0,b)}$ is experimental. Note, however, that the uncertainty in $A_{FB}^{(0,b)}$ is strongly statistics dominated. The combined value, $A_b = 0.899 \pm 0.013$ deviates by 2.8σ . It would be difficult to account for this 4.0% deviation by new physics that enters only at the level of radiative corrections since about a 20% correction to $\hat{\kappa}_b$ would be necessary to account for the central value of A_b [211]. If this deviation is due to new physics, it is most likely of tree-level type affecting preferentially the third generation. Examples include the decay of a scalar neutrino resonance [209], mixing of the b quark with heavy exotics [210], and a heavy Z' with family-nonuniversal couplings [212,213]. It is difficult, however, to simultaneously account for R_b , which has been measured on the Z peak and off-peak [214] at LEP 1. An average of R_b measurements at LEP 2 at energies between 133 and 207 GeV is 2.1σ below the SM prediction, while $A_{FB}^{(b)}$ (LEP 2) is 1.6σ low [160].

The left-right asymmetry, $A_{LR}^0 = 0.15138 \pm 0.00216$ [152], based on all hadronic data from 1992–1998 differs 1.8σ from the SM expectation of 0.1475 ± 0.0010 . The combined value of $A_\ell = 0.1513 \pm 0.0021$ from SLD (using lepton-family universality and including correlations) is also 1.8σ above the SM prediction; but there is now experimental agreement between this SLD value and the LEP 1 value, $A_\ell = 0.1481 \pm 0.0027$, obtained from a fit to $A_{FB}^{(0,\ell)}$, $A_e(\mathcal{P}_\tau)$, and $A_\tau(\mathcal{P}_\tau)$, again assuming universality.

The observables in Table 10.6 and Table 10.7, as well as some other less precise observables, are used in the global fits described below. In all fits, the errors include full statistical, systematic, and theoretical uncertainties. The correlations on the LEP 1 lineshape and τ polarization, the LEP/SLD heavy flavor observables, the SLD lepton asymmetries, and the deep inelastic and ν - e scattering observables, are included. The theoretical correlations between $\Delta\alpha_{\text{had}}^{(5)}$ and $g_\mu - 2$, and between the charm and bottom quark masses, are also accounted for.

The data allow a simultaneous determination of M_Z , M_H , m_t , and the strong coupling $\alpha_s(M_Z)$. (\hat{m}_c , \hat{m}_b , and $\Delta\alpha_{\text{had}}^{(3)}$ are also allowed to float in the fits, subject to the theoretical constraints [5,17] described in Sec. 10.1–Sec. 10.2. These are correlated with α_s .) α_s is determined mainly from R_ℓ , Γ_Z , σ_{had} , and τ_τ and is only weakly correlated with the other variables. The global fit to all data, including the CDF/DØ average $m_t = 173.1 \pm 1.3$ GeV, yields the result in Table 10.5 (the $\overline{\text{MS}}$ top quark mass given there corresponds to $m_t = 173.2 \pm 1.3$ GeV). The weak mixing angle is determined to

$$\hat{s}_Z^2 = 0.23116 \pm 0.00013, \quad s_W^2 = 0.22292 \pm 0.00028,$$

where the larger error in the on-shell scheme is due to the stronger sensitivity to m_t , while the corresponding effective angle is related by Eq. (10.34), *i.e.*, $\overline{s}_\ell^2 = 0.23146 \pm 0.00012$.

[†] Alternatively, one can use $A_\ell = 0.1481 \pm 0.0027$, which is from LEP 1 alone and in excellent agreement with the SM, and obtain $A_b = 0.893 \pm 0.022$ which is 1.9σ low. This illustrates that some of the discrepancy is related to the one in A_{LR} .

As described at the beginning of Sec. 10.2 and the paragraph following Eq. (10.42) in Sec. 10.5, there is considerable stress in the experimental e^+e^- spectral functions and also conflict when these are compared with τ decay spectral functions. These are below or above the 2σ level (depending on what is actually compared) but not larger than the deviations of some other quantities entering our analyzes. The number and size of these deviations are not inconsistent with what one would expect to happen as a result of random fluctuations. It is nevertheless instructive to study the effect of doubling the uncertainty in $\Delta\alpha_{\text{had}}^{(3)}(1.8 \text{ GeV}) = (57.29 \pm 0.90) \times 10^{-4}$, (see the beginning of Sec. 10.2) on the extracted Higgs mass. The result, $M_H = 87_{-22}^{+28} \text{ GeV}$, demonstrates that the uncertainty in $\Delta\alpha_{\text{had}}$ is currently of only secondary importance. Note also, that the uncertainty of about ± 0.0001 in $\Delta\alpha_{\text{had}}^{(3)}(1.8 \text{ GeV})$ corresponds to a shift of $\mp 5 \text{ GeV}$ in M_H or about one fifth of its total uncertainty. The hadronic contribution to $\alpha(M_Z)$ is correlated with $g_\mu - 2$ (see Sec. 10.5). The measurement of the latter is higher than the SM prediction, and its inclusion in the fit favors a larger $\alpha(M_Z)$ and a lower M_H (currently by about 2 GeV).

The weak mixing angle can be determined from Z pole observables, M_W , and from a variety of neutral-current processes spanning a very wide Q^2 range. The results (for the older low energy neutral-current data see Refs. 58 and 59) shown in Table 10.8 are in reasonable agreement with each other, indicating the quantitative success of the SM. The largest discrepancy is the value $\hat{s}_Z^2 = 0.23193 \pm 0.00028$ from the forward-backward asymmetries into bottom and charm quarks, which is 2.7σ above the value 0.23116 ± 0.00013 from the global fit to all data. Similarly, $\hat{s}_Z^2 = 0.23067 \pm 0.00029$ from the SLD asymmetries (in both cases when combined with M_Z) is 1.7σ low. The SLD result has the additional difficulty (within the SM) of implying very low and excluded [161] Higgs masses. This is also true for $\hat{s}_Z^2 = 0.23100 \pm 0.00023$ from M_W and M_Z and — as a consequence — for the global fit. We have therefore included in Table 10.6 and Table 10.7 an additional column (denoted Deviation) indicating the deviations if $M_H = 117 \text{ GeV}$ is fixed.

The extracted Z pole value of $\alpha_s(M_Z)$ is based on a formula with negligible theoretical uncertainty if one assumes the exact validity of the SM. One should keep in mind, however, that this value, $\alpha_s(M_Z) = 0.1198 \pm 0.0028$, is very sensitive to such types of new physics as non-universal vertex corrections. In contrast, the value derived from τ decays, $\alpha_s(M_Z) = 0.1174_{-0.0016}^{+0.0018}$, is theory dominated but less sensitive to new physics. The two values are in remarkable agreement with each other. They are also in agreement with other recent values, such as from jet-event shapes at LEP [215] (0.1202 ± 0.0050) the average from HERA [216] (0.1198 ± 0.0032), and the most recent unquenched lattice calculation [217] (0.1183 ± 0.0008). For more details and other determinations, see our Section 9 on “Quantum Chromodynamics” in this *Review*.

Using $\alpha(M_Z)$ and \hat{s}_Z^2 as inputs, one can predict $\alpha_s(M_Z)$ assuming grand unification. One predicts [218] $\alpha_s(M_Z) = 0.130 \pm 0.001 \pm 0.01$ for the simplest theories based on the minimal supersymmetric extension of the SM, where the first (second) uncertainty is from the inputs (thresholds). This is slightly larger, but consistent with the experimental $\alpha_s(M_Z) = 0.1183 \pm 0.0015$ from the Z lineshape and the τ lifetime, as well as

Table 10.8: Values of \hat{s}_Z^2 , s_W^2 , α_s , and M_H [in GeV] for various (combinations of) observables. Unless indicated otherwise, the top quark mass, $m_t = 170.9 \pm 1.9$ GeV, is used as an additional constraint in the fits. The (\dagger) symbol indicates a fixed parameter.

Data	\hat{s}_Z^2	s_W^2	$\alpha_s(M_Z)$	M_H
All data	0.23116(13)	0.22292(28)	0.1183(15)	90_{-22}^{+27}
All indirect (no m_t)	0.23118(14)	0.22283(34)	0.1183(16)	112_{-52}^{+110}
Z pole (no m_t)	0.23121(17)	0.22311(59)	0.1198(28)	90_{-44}^{+114}
LEP 1 (no m_t)	0.23152(21)	0.22376(67)	0.1213(30)	170_{-93}^{+234}
SLD + M_Z	0.23067(29)	0.22201(54)	0.1183 (\dagger)	33_{-17}^{+27}
$A_{FB}^{(b,c)} + M_Z$	0.23193(28)	0.22484(76)	0.1183 (\dagger)	389_{-158}^{+264}
$M_W + M_Z$	0.23100(23)	0.22262(48)	0.1183 (\dagger)	67_{-28}^{+38}
M_Z	0.23128(6)	0.22321(17)	0.1183 (\dagger)	117 (\dagger)
Q_W (APV)	0.2314(14)	0.2233(14)	0.1183 (\dagger)	117 (\dagger)
$Q_W(e)$	0.2332(15)	0.2251(15)	0.1183 (\dagger)	117 (\dagger)
ν_μ -N DIS (isoscalar)	0.2335(18)	0.2254(18)	0.1183 (\dagger)	117 (\dagger)
Elastic $\nu_\mu(\bar{\nu}_\mu)$ - e	0.2311(77)	0.2230(77)	0.1183 (\dagger)	117 (\dagger)
e -D DIS (SLAC)	0.222(18)	0.213(19)	0.1183 (\dagger)	117 (\dagger)
Elastic $\nu_\mu(\bar{\nu}_\mu)$ - p	0.211(33)	0.203(33)	0.1183 (\dagger)	117 (\dagger)

with other determinations. Non-supersymmetric unified theories predict the low value $\alpha_s(M_Z) = 0.073 \pm 0.001 \pm 0.001$. See also the note on ‘‘Supersymmetry’’ in the Searches Particle Listings.

The data indicate a preference for a small Higgs mass. There is a strong correlation between the quadratic m_t and logarithmic M_H terms in $\hat{\rho}$ in all of the indirect data except for the $Z \rightarrow b\bar{b}$ vertex. Therefore, observables (other than R_b) which favor m_t values higher than the Tevatron range favor lower values of M_H . M_W has additional M_H dependence through $\Delta\hat{r}_W$ which is not coupled to m_t^2 effects. The strongest individual pulls toward smaller M_H are from M_W and A_{LR}^0 , while $A_{FB}^{(0,b)}$ favors higher values. The difference in χ^2 for the global fit is $\Delta\chi^2 = \chi^2(M_H = 300 \text{ GeV}) - \chi_{\min}^2 \approx 25$. Hence, the data favor a small value of M_H , as in supersymmetric extensions of the SM. The central value of the global fit result, $M_H = 90_{-22}^{+27}$ GeV, is below the direct lower bound, $M_H \geq 114.4$ GeV (95% CL) [161].

The 90% central confidence range from all precision data is

$$55 \text{ GeV} \leq M_H \leq 135 \text{ GeV}. \quad (10.44)$$

Including the results of the direct searches at LEP 2 [161] and the Tevatron [219] as extra contributions to the likelihood function drives the 95% upper limit to $M_H \leq 147 \text{ GeV}$. As two further refinements, we account for (i) theoretical uncertainties from uncalculated higher order contributions by allowing the T parameter (see next subsection) subject to the constraint $T = 0 \pm 0.02$, (ii) the M_H dependence of the correlation matrix which gives slightly more weight to lower Higgs masses [220]. The resulting limits at 95 (90, 99)% CL are, respectively,

$$M_H \leq 149 \text{ (145, 194) GeV}. \quad (10.45)$$

One can also carry out a fit to the indirect data alone, *i.e.*, without including the constraint, $m_t = 173.1 \pm 1.3 \text{ GeV}$, obtained by CDF and DØ. (The indirect prediction is for the $\overline{\text{MS}}$ mass, $\widehat{m}_t(\widehat{m}_t) = 166.2_{-6.6}^{+8.1} \text{ GeV}$, which is in the end converted to the pole mass). One obtains $m_t = 176.0_{-7.0}^{+8.5} \text{ GeV}$, in perfect agreement with the direct CDF/DØ average. Using this indirect top mass value, the tendency for a light Higgs persists and Eq. (10.44) becomes $46 \text{ GeV} \leq M_H \leq 306 \text{ GeV}$. The relations between M_H and m_t for various observables are shown in Fig. 10.2.

One can also determine the radiative correction parameters Δr : from the global fit one obtains $\Delta r = 0.0351 \pm 0.0009$ and $\Delta \widehat{r}_W = 0.06950 \pm 0.00021$. M_W measurements [160,207] (when combined with M_Z) are equivalent to measurements of $\Delta r = 0.0342 \pm 0.0014$, which is 0.9σ below the result from all other data, $\Delta r = 0.0357 \pm 0.0011$. Fig. 10.3 shows the 1σ contours in the M_W - m_t plane from the direct and indirect determinations, as well as the combined 90% CL region. The indirect determination uses M_Z from LEP 1 as input, which is defined assuming an s -dependent decay width. M_W then corresponds to the s -dependent width definition, as well, and can be directly compared with the results from the Tevatron and LEP 2 which have been obtained using the same definition. The difference to a constant width definition is formally only of $\mathcal{O}(\alpha^2)$, but is strongly enhanced since the decay channels add up coherently. It is about 34 MeV for M_Z and 27 MeV for M_W . The residual difference between working consistently with one or the other definition is about 3 MeV, *i.e.*, of typical size for non-enhanced $\mathcal{O}(\alpha^2)$ corrections [72–75].

Most of the parameters relevant to ν -hadron, ν - e , e -hadron, and e^-e^\pm processes are determined uniquely and precisely from the data in “model-independent” fits (*i.e.*, fits which allow for an arbitrary electroweak gauge theory). The values for the parameters defined in Eqs. (10.11)–(10.14) are given in Table 10.9 along with the predictions of the SM. The agreement is very good. (The ν -hadron results without the NuTeV data can be found in the 1998 edition of this *Review*, and the fits using the original NuTeV data in the 2006 edition.) The off Z pole e^+e^- results are difficult to present in a model-independent way because Z propagator effects are non-negligible at TRISTAN, PETRA, PEP, and LEP 2 energies. However, assuming e - μ - τ universality, the low energy lepton asymmetries imply [150] $4(g_A^e)^2 = 0.99 \pm 0.05$, in good agreement with the SM prediction $\simeq 1$.

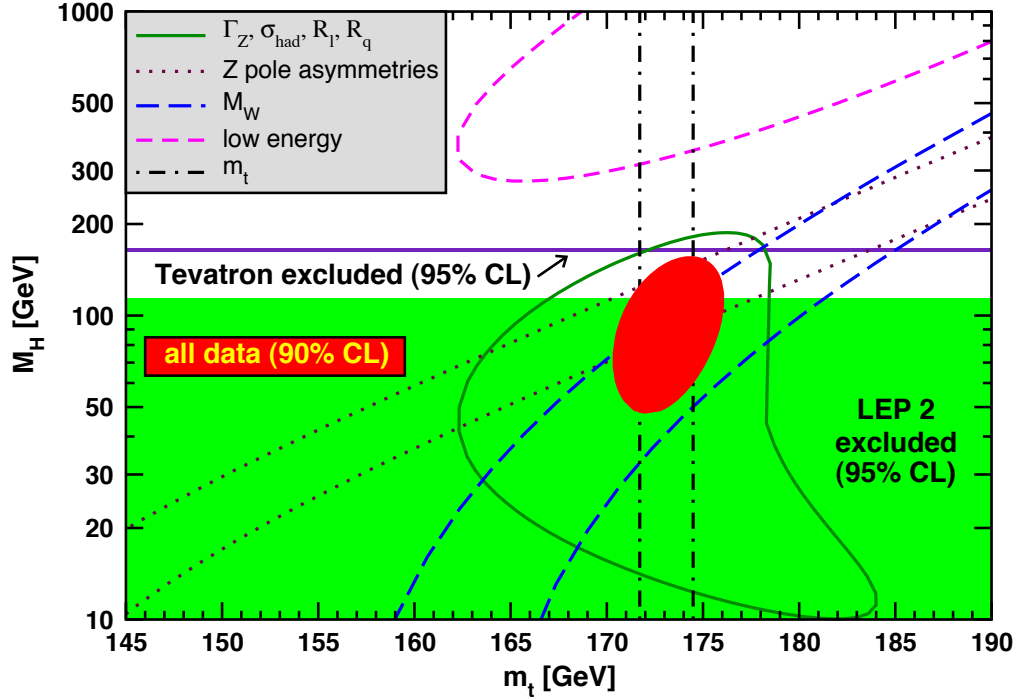


Figure 10.2: One-standard-deviation (39.35%) uncertainties in M_H as a function of m_t for various inputs, and the 90% CL region ($\Delta\chi^2 = 4.605$) allowed by all data. $\alpha_s(M_Z) = 0.1183$ is assumed except for the fits including the Z lineshape or low energy data. The direct lower limit from LEP 2 and the excluded window from the Tevatron [221] (both at the 95% CL) are also shown. Color version at end of book.

10.7. Constraints on new physics

The Z pole, W mass, and low energy data can be used to search for and set limits on deviations from the SM. In particular, the combination of these indirect data with the direct CDF and $D\bar{O}$ average for m_t allows one to set stringent limits on new physics. We will mainly discuss the effects of exotic particles (with heavy masses $M_{\text{new}} \gg M_Z$ in an expansion in M_Z/M_{new}) on the gauge boson self-energies. (Brief remarks are made on new physics which is not of this type.) Most of the effects on precision measurements can be described by three gauge self-energy parameters S , T , and U . We will define these, as well as related parameters, such as ρ_0 , ϵ_i , and $\hat{\epsilon}_i$, to arise from new physics only. *I.e.*, they are equal to zero ($\rho_0 = 1$) exactly in the SM, and do not include any contributions from m_t or M_H , which are treated separately. Our treatment differs from most of the original papers.

Many extensions of the SM can be described by the ρ_0 parameter,

$$\rho_0 \equiv \frac{M_W^2}{M_Z^2 \hat{c}_Z^2 \hat{\rho}}, \quad (10.46)$$

which describes new sources of SU(2) breaking that cannot be accounted for by the SM

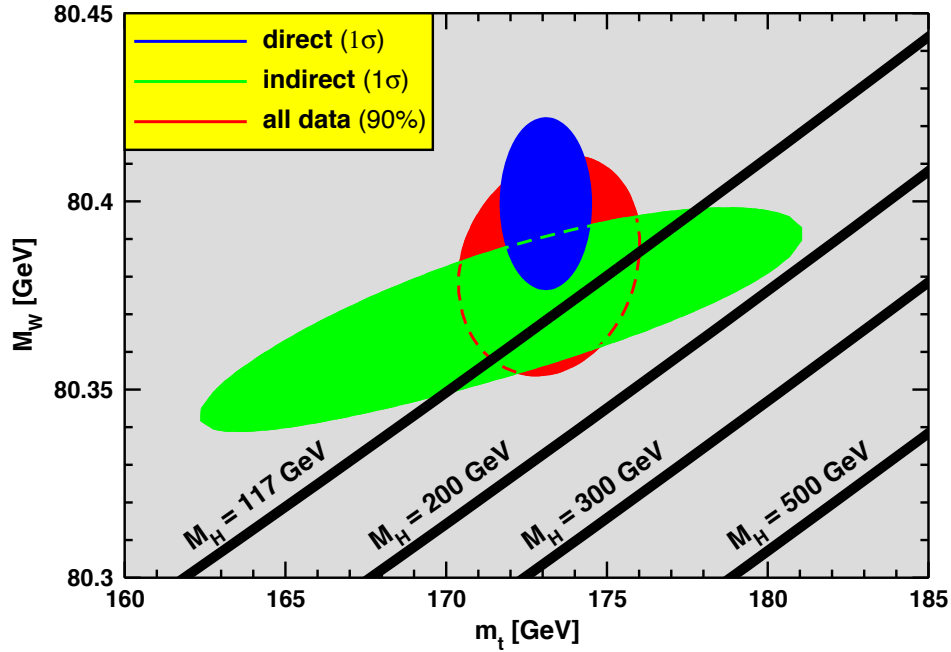


Figure 10.3: One-standard-deviation (39.35%) region in M_W as a function of m_t for the direct and indirect data, and the 90% CL region ($\Delta\chi^2 = 4.605$) allowed by all data. The SM prediction as a function of M_H is also indicated. The widths of the M_H bands reflect the theoretical uncertainty from $\alpha(M_Z)$. Color version at end of book.

Higgs doublet or m_t effects. In the presence of $\rho_0 \neq 1$, Eq. (10.46) generalizes the second Eq. (10.8) while the first remains unchanged. Provided that the new physics which yields $\rho_0 \neq 1$ is a small perturbation which does not significantly affect the radiative corrections, ρ_0 can be regarded as a phenomenological parameter which multiplies G_F in Eqs. (10.11)–(10.14), (10.28), and Γ_Z in Eq. (10.36c). There are enough data to determine ρ_0 , M_H , m_t , and α_s , simultaneously. From the global fit,

$$\rho_0 = 1.0008^{+0.0017}_{-0.0007}, \quad (10.47)$$

$$114.4 \text{ GeV} \leq M_H \leq 427 \text{ GeV}, \quad (10.48)$$

$$m_t = 173.1 \pm 1.3 \text{ GeV}, \quad (10.49)$$

$$\alpha_s(M_Z) = 0.1181 \pm 0.0015, \quad (10.50)$$

where the lower limit on M_H is the direct search bound. (If the direct limit is ignored one obtains $M_H = 162^{+265}_{-93}$ GeV and $\rho_0 = 1.0008^{+0.0017}_{-0.0010}$.) The error bar in Eq. (10.47) is highly asymmetric: at the 2σ level one has $\rho_0 = 1.0004^{+0.0029}_{-0.0011}$ with no meaningful bound on M_H . The result in Eq. (10.47) is slightly above but consistent with the SM expectation, $\rho_0 = 1$. It can be used to constrain higher-dimensional Higgs representations to have vacuum expectation values of less than a few percent of those of the doublets. Indeed, the relation between M_W and M_Z is modified if there are Higgs multiplets with

Table 10.9: Values of the model-independent neutral-current parameters, compared with the SM predictions. There is a second $g_{V,A}^{\nu e}$ solution, given approximately by $g_V^{\nu e} \leftrightarrow g_A^{\nu e}$, which is eliminated by e^+e^- data under the assumption that the neutral current is dominated by the exchange of a single Z boson. The ϵ_L , as well as the ϵ_R , are strongly correlated and non-Gaussian, so that for implementations we recommend the parametrization using g_i^2 and $\theta_i = \tan^{-1}[\epsilon_i(u)/\epsilon_i(d)]$, $i = L$ or R . The analysis of more recent low energy experiments in polarized electron scattering performed in Ref. 123 is included by means of the two orthogonal constraints, $\cos \gamma C_{1d} - \sin \gamma C_{1u} = 0.342 \pm 0.063$ and $\sin \gamma C_{1d} + \cos \gamma C_{1u} = -0.0285 \pm 0.0043$, where $\tan \gamma \approx 0.445$. In the SM predictions, the uncertainty is from M_Z , M_H , m_t , m_b , m_c , $\hat{\alpha}(M_Z)$, and α_s .

Quantity	Experimental Value	SM	Correlation		
$\epsilon_L(u)$	0.338 ± 0.016	0.3461(1)			
$\epsilon_L(d)$	-0.434 ± 0.012	-0.4292(1)	non-		
$\epsilon_R(u)$	$-0.174 \begin{smallmatrix} +0.013 \\ -0.004 \end{smallmatrix}$	-0.1549(1)	Gaussian		
$\epsilon_R(d)$	$-0.023 \begin{smallmatrix} +0.071 \\ -0.047 \end{smallmatrix}$	0.0775			
g_L^2	0.3025 ± 0.0014	0.3040(2)	-0.18	-0.21	-0.02
g_R^2	0.0309 ± 0.0010	0.0300		-0.03	-0.07
θ_L	2.48 ± 0.036	2.4630(1)			0.24
θ_R	$4.58 \begin{smallmatrix} +0.41 \\ -0.28 \end{smallmatrix}$	5.1765			
$g_V^{\nu e}$	-0.040 ± 0.015	-0.0398(3)			-0.05
$g_A^{\nu e}$	-0.507 ± 0.014	-0.5064(1)			
$C_{1u} + C_{1d}$	0.1537 ± 0.0011	0.1528(1)	0.64	-0.18	-0.01
$C_{1u} - C_{1d}$	-0.516 ± 0.014	-0.5300(3)		-0.27	-0.02
$C_{2u} + C_{2d}$	-0.21 ± 0.57	-0.0089			-0.30
$C_{2u} - C_{2d}$	-0.077 ± 0.044	-0.0625(5)			
$Q_W(e) = -2C_{2e}$	-0.0403 ± 0.0053	-0.0473(5)			

weak isospin $> 1/2$ with significant vacuum expectation values. In order to calculate to higher orders in such theories one must define a set of four fundamental renormalized parameters which one may conveniently choose to be α , G_F , M_Z , and M_W , since M_W and M_Z are directly measurable. Then \hat{s}_Z^2 and ρ_0 can be considered dependent parameters.

Eq. (10.47) can also be used to constrain other types of new physics. For example,

non-degenerate multiplets of heavy fermions or scalars break the vector part of weak SU(2) and lead to a decrease in the value of M_Z/M_W . A non-degenerate SU(2) doublet $\begin{pmatrix} f_1 \\ f_2 \end{pmatrix}$ yields a positive contribution to ρ_0 [222] of

$$\frac{C G_F}{8\sqrt{2}\pi^2} \Delta m^2, \quad (10.51)$$

where

$$\Delta m^2 \equiv m_1^2 + m_2^2 - \frac{4m_1^2 m_2^2}{m_1^2 - m_2^2} \ln \frac{m_1}{m_2} \geq (m_1 - m_2)^2, \quad (10.52)$$

and $C = 1$ (3) for color singlets (triplets). Thus, in the presence of such multiplets,

$$\rho_0 = 1 + \frac{3 G_F}{8\sqrt{2}\pi^2} \sum_i \frac{C_i}{3} \Delta m_i^2, \quad (10.53)$$

where the sum includes fourth-family quark or lepton doublets, $\begin{pmatrix} t' \\ b' \end{pmatrix}$ or $\begin{pmatrix} E^0 \\ E^- \end{pmatrix}$, and scalar doublets such as $\begin{pmatrix} \tilde{t} \\ \tilde{b} \end{pmatrix}$ in Supersymmetry (in the absence of L - R mixing). This implies

$$\sum_i \frac{C_i}{3} \Delta m_i^2 \leq (106 \text{ GeV})^2 \quad (10.54)$$

at 95% CL. The corresponding constraints on non-degenerate squark and slepton doublets are even stronger, $\sum_i C_i \Delta m_i^2 / 3 \leq (61 \text{ GeV})^2$. This is due to the supersymmetric Higgs mass bound, $m_{h0} < 150 \text{ GeV}$, and the very strong correlation between m_{h0} and ρ_0 (97%).

Non-degenerate multiplets usually imply $\rho_0 > 1$. Similarly, heavy Z' bosons decrease the prediction for M_Z due to mixing and generally lead to $\rho_0 > 1$ [223]. On the other hand, additional Higgs doublets which participate in spontaneous symmetry breaking [224], heavy lepton doublets involving Majorana neutrinos [225], and the vacuum expectation values of Higgs triplets or higher-dimensional representations can contribute to ρ_0 with either sign. Allowing for the presence of heavy degenerate chiral multiplets (the S parameter, to be discussed below) affects the determination of ρ_0 from the data, at present leading to a larger value (for fixed M_H).

A number of authors [226–231] have considered the general effects on neutral-current and Z and W boson observables of various types of heavy (*i.e.*, $M_{\text{new}} \gg M_Z$) physics which contribute to the W and Z self-energies but which do not have any direct coupling to the ordinary fermions. In addition to non-degenerate multiplets, which break the vector part of weak SU(2), these include heavy degenerate multiplets of chiral fermions which break the axial generators. The effects of one degenerate chiral doublet are small, but in Technicolor theories there may be many chiral doublets and therefore significant effects [226].

Such effects can be described by just three parameters, S , T , and U , at the (electroweak) one-loop level. (Three additional parameters are needed if the new physics

36 10. Electroweak model and constraints on new physics

scale is comparable to M_Z [232]. Further generalizations, including effects relevant to LEP 2, are described in Ref. 233.) T is proportional to the difference between the W and Z self-energies at $Q^2 = 0$ (*i.e.*, vector SU(2)-breaking), while S ($S + U$) is associated with the difference between the Z (W) self-energy at $Q^2 = M_{Z,W}^2$ and $Q^2 = 0$ (axial SU(2)-breaking). Denoting the contributions of new physics to the various self-energies by Π_{ij}^{new} , we have

$$\hat{\alpha}(M_Z)T \equiv \frac{\Pi_{WW}^{\text{new}}(0)}{M_W^2} - \frac{\Pi_{ZZ}^{\text{new}}(0)}{M_Z^2}, \quad (10.55a)$$

$$\begin{aligned} \frac{\hat{\alpha}(M_Z)}{4\hat{s}_Z^2\hat{c}_Z^2}S &\equiv \frac{\Pi_{ZZ}^{\text{new}}(M_Z^2) - \Pi_{ZZ}^{\text{new}}(0)}{M_Z^2} - \\ &\frac{\hat{c}_Z^2 - \hat{s}_Z^2}{\hat{c}_Z\hat{s}_Z} \frac{\Pi_{Z\gamma}^{\text{new}}(M_Z^2)}{M_Z^2} - \frac{\Pi_{\gamma\gamma}^{\text{new}}(M_Z^2)}{M_Z^2}, \end{aligned} \quad (10.55b)$$

$$\begin{aligned} \frac{\hat{\alpha}(M_Z)}{4\hat{s}_Z^2}(S + U) &\equiv \frac{\Pi_{WW}^{\text{new}}(M_W^2) - \Pi_{WW}^{\text{new}}(0)}{M_W^2} - \\ &\frac{\hat{c}_Z}{\hat{s}_Z} \frac{\Pi_{Z\gamma}^{\text{new}}(M_Z^2)}{M_Z^2} - \frac{\Pi_{\gamma\gamma}^{\text{new}}(M_Z^2)}{M_Z^2}. \end{aligned} \quad (10.55c)$$

S , T , and U are defined with a factor proportional to $\hat{\alpha}$ removed, so that they are expected to be of order unity in the presence of new physics. In the $\overline{\text{MS}}$ scheme as defined in Ref. 64, the last two terms in Eqs. (10.55b) and (10.55c) can be omitted (as was done in some earlier editions of this *Review*). These three parameters are related to other parameters (S_i , h_i , $\hat{\epsilon}_i$) defined in Refs. [64,227,228] by

$$\begin{aligned} T &= h_V = \hat{\epsilon}_1/\hat{\alpha}(M_Z), \\ S &= h_{AZ} = S_Z = 4\hat{s}_Z^2\hat{\epsilon}_3/\hat{\alpha}(M_Z), \\ U &= h_{AW} - h_{AZ} = S_W - S_Z = -4\hat{s}_Z^2\hat{\epsilon}_2/\hat{\alpha}(M_Z). \end{aligned} \quad (10.56)$$

A heavy non-degenerate multiplet of fermions or scalars contributes positively to T as

$$\rho_0 - 1 = \frac{1}{1 - \hat{\alpha}(M_Z)T} - 1 \simeq \hat{\alpha}(M_Z)T, \quad (10.57)$$

where ρ_0 is given in Eq. (10.53). The effects of non-standard Higgs representations cannot be separated from heavy non-degenerate multiplets unless the new physics has other consequences, such as vertex corrections. Most of the original papers defined T to include the effects of loops only. However, we will redefine T to include all new sources of SU(2) breaking, including non-standard Higgs, so that T and ρ_0 are equivalent by Eq. (10.57).

A multiplet of heavy degenerate chiral fermions yields

$$S = \frac{C}{3\pi} \sum_i \left(t_{3L}(i) - t_{3R}(i) \right)^2, \quad (10.58)$$

where $t_{3L,R}(i)$ is the third component of weak isospin of the left-(right-)handed component of fermion i and C is the number of colors. For example, a heavy degenerate ordinary or mirror family would contribute $2/3\pi$ to S . In Technicolor models with QCD-like dynamics, one expects [226] $S \sim 0.45$ for an iso-doublet of techni-fermions, assuming $N_{TC} = 4$ techni-colors, while $S \sim 1.62$ for a full techni-generation with $N_{TC} = 4$; T is harder to estimate because it is model-dependent. In these examples one has $S \geq 0$. However, the QCD-like models are excluded on other grounds (flavor changing neutral-currents, and too-light quarks and pseudo-Goldstone bosons [234]). In particular, these estimates do not apply to models of walking Technicolor [234], for which S can be smaller or even negative [235]. Other situations in which $S < 0$, such as loops involving scalars or Majorana particles, are also possible [236]. The simplest origin of $S < 0$ would probably be an additional heavy Z' boson [223], which could mimic $S < 0$. Supersymmetric extensions of the SM generally give very small effects. See Refs. 181 and 237 and the note on ‘‘Supersymmetry’’ in the Searches Particle Listings for a complete set of references.

Most simple types of new physics yield $U = 0$, although there are counter-examples, such as the effects of anomalous triple gauge vertices [228].

The SM expressions for observables are replaced by

$$\begin{aligned} M_Z^2 &= M_{Z0}^2 \frac{1 - \hat{\alpha}(M_Z)T}{1 - G_F M_{Z0}^2 S / 2\sqrt{2}\pi}, \\ M_W^2 &= M_{W0}^2 \frac{1}{1 - G_F M_{W0}^2 (S + U) / 2\sqrt{2}\pi}, \end{aligned} \quad (10.59)$$

where M_{Z0} and M_{W0} are the SM expressions (as functions of m_t and M_H) in the $\overline{\text{MS}}$ scheme. Furthermore,

$$\Gamma_Z = \frac{M_Z^3 \beta_Z}{1 - \hat{\alpha}(M_Z)T}, \quad \Gamma_W = M_W^3 \beta_W, \quad A_i = \frac{A_{i0}}{1 - \hat{\alpha}(M_Z)T}, \quad (10.60)$$

where β_Z and β_W are the SM expressions for the reduced widths Γ_{Z0}/M_{Z0}^3 and Γ_{W0}/M_{W0}^3 , M_Z and M_W are the physical masses, and A_i (A_{i0}) is a neutral-current amplitude (in the SM).

The data allow a simultaneous determination of \hat{s}_Z^2 (from the Z pole asymmetries), S (from M_Z), U (from M_W), T (mainly from Γ_Z), α_s (from R_ℓ , σ_{had} , and τ_τ), and m_t (from CDF and DØ), with little correlation among the SM parameters:

$$\begin{aligned} S &= 0.01 \pm 0.10 (-0.08), \\ T &= 0.03 \pm 0.11 (+0.09), \\ U &= 0.06 \pm 0.10 (+0.01), \end{aligned} \quad (10.61)$$

38 10. Electroweak model and constraints on new physics

and $\hat{s}_Z^2 = 0.23124 \pm 0.00016$, $\alpha_s(M_Z) = 0.1183 \pm 0.0016$, $m_t = 173.0 \pm 1.3$ GeV, where the uncertainties are from the inputs. The central values assume $M_H = 117$ GeV and in parentheses we show the difference to assuming $M_H = 300$ GeV instead. As can be seen, the SM parameters (U) can be determined with no (little) M_H dependence. On the other hand, S , T , and M_H cannot be obtained simultaneously, because the Higgs boson loops themselves are resembled approximately by oblique effects. Eqs. (10.61) show that negative (positive) contributions to the S (T) parameter can weaken or entirely remove the strong constraints on M_H from the SM fits. Specific models in which a large M_H is compensated by new physics are reviewed in Ref. 238. The parameters in Eqs. (10.61), which by definition are due to new physics only, are in reasonable agreement with the SM values of zero. Fixing $U = 0$ (as is also done in Fig. 10.4) moves S and T slightly upwards,

$$\begin{aligned} S &= 0.03 \pm 0.09 (-0.07), \\ T &= 0.07 \pm 0.08 (+0.09). \end{aligned} \tag{10.62}$$

The correlation between S and T in this fit amounts to 87%.

Using Eq. (10.57), the value of ρ_0 corresponding to T in Eq. (10.61) is $1.0002 \pm 0.0009 (+0.0007)$, while the one corresponding to Eq. (10.62) is $1.0006 \pm 0.0006 (+0.0007)$. The values of the $\hat{\epsilon}$ parameters defined in Eq. (10.56) are

$$\begin{aligned} \hat{\epsilon}_3 &= 0.0000 \pm 0.0009 (-0.0006), \\ \hat{\epsilon}_1 &= 0.0002 \pm 0.0008 (+0.0007), \\ \hat{\epsilon}_2 &= -0.0005 \pm 0.0009 (-0.0001). \end{aligned} \tag{10.63}$$

Unlike the original definition, we defined the quantities in Eqs. (10.63) to vanish identically in the absence of new physics and to correspond directly to the parameters S , T , and U in Eqs. (10.61). There is a strong correlation (88%) between the S and T parameters. The allowed regions in S - T are shown in Fig. 10.4. From Eqs. (10.61) one obtains $S \leq 0.16$ (0.08) and $T \leq 0.21$ (0.29) at 95% CL for $M_H = 117$ GeV (300 GeV). If one fixes $M_H = 600$ GeV and requires the constraint $S \geq 0$ (as is appropriate in QCD-like Technicolor models) then $S \leq 0.13$ (Bayesian) or $S \leq 0.10$ (frequentist). This rules out simple Technicolor models with many techni-doublets and QCD-like dynamics.

An extra generation of SM fermions is excluded at the 6σ level on the basis of the S parameter alone, corresponding to $N_F = 2.85 \pm 0.20$ for the number of families. This result assumes that there are no new contributions to T or U and therefore that any new families are degenerate, and is in agreement with a fit to the number of light neutrinos, $N_\nu = 2.991 \pm 0.007$. However, the S parameter fits are valid even for a very heavy fourth family neutrino. This restriction can be relaxed by allowing T to vary as well, since $T > 0$ is expected from a non-degenerate extra family. Fixing $S = 2/3\pi$, the global fit favors a fourth family contribution to T of 0.22 ± 0.04 . However, the quality of the fit deteriorates ($\Delta\chi^2 = 3.2$ relative to the SM fit with M_H forced not to drop below its LEP 2 bound of 114.4 GeV) so that this tuned T scenario is also disfavored but only at about the 90%

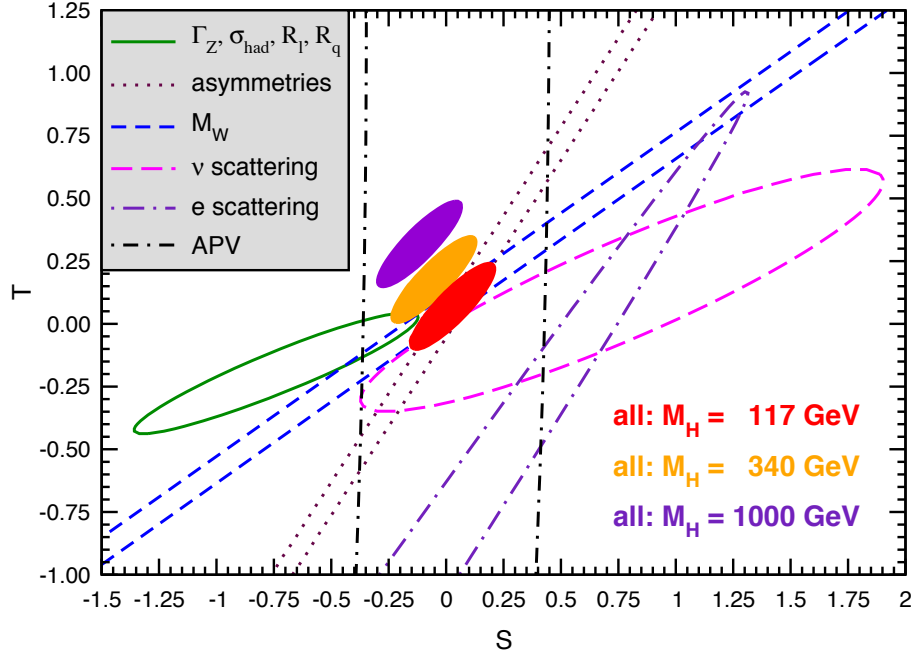


Figure 10.4: 1σ constraints (39.35%) on S and T from various inputs combined with M_Z . S and T represent the contributions of new physics only. (Uncertainties from m_t are included in the errors.) The contours assume $M_H = 117$ GeV except for the central and upper 90% CL contours allowed by all data, which are for $M_H = 340$ GeV and 1000 GeV, respectively. Data sets not involving M_W are insensitive to U . Due to higher order effects, however, $U = 0$ has to be assumed in all fits. α_s is constrained using the τ lifetime as additional input in all fits. Because this has changed significantly since the 2008 edition of this *Review* (see the discussion in Sec. 10.5), the strongly α_s -dependent solid (green) contour from Z lineshape and cross-section measurements has moved significantly towards negative S and T . The long-dashed (magenta) contour from ν scattering has moved closer towards the global averages (see Sec. 10.3). The long-dash-dotted (indigo) contour from polarized e scattering [123,125] is the upper tip of an elongated ellipse centered at around $S = -15$ and $T = -21$. At first sight it looks as if it is deviating strongly but it is off by only 1.8σ . This illusion arises because $\Delta\chi^2 > 0.8$ everywhere on the visible part of the contour. Color version at end of book.

CL which is weaker compared to the 2008 edition of this *Review*, *i.e.* before the latest developments in APV and the ν -DIS interpretation. In fact, tuned mass splittings of the extra leptons and quarks [239] can now yield fits with only moderately higher χ^2 values (by about 1 unit) than for the SM. A more detailed analysis is also required if the extra neutrino (or the extra down-type quark) is close to its direct mass limit [240]. Thus, a fourth family is disfavored but not excluded by current data. Similar remarks apply to a heavy mirror family [241] involving right-handed SU(2) doublets and left-handed singlets. A more detailed discussion based on the same data set as used for this *Review* can be

found in Ref. 242. Additional heavy ordinary or mirror generations may also require large Yukawa and Higgs couplings that may lead to Landau poles at low scales [243]. In contrast, heavy degenerate non-chiral (also known as vector-like or exotic) multiplets, which are predicted in many grand unified theories [244] and other extensions of the SM, do not contribute to S , T , and U (or to ρ_0), and do not require large coupling constants. Such exotic multiplets may occur in partial families, as in E_6 models, or as complete vector-like families [245].

There is no simple parametrization to describe the effects of every type of new physics on every possible observable. The S , T , and U formalism describes many types of heavy physics which affect only the gauge self-energies, and it can be applied to all precision observables. However, new physics which couples directly to ordinary fermions, such as heavy Z' bosons [223], mixing with exotic fermions [246], or leptoquark exchange [160,247] cannot be fully parametrized in the S , T , and U framework. It is convenient to treat these types of new physics by parameterizations that are specialized to that particular class of theories (*e.g.*, extra Z' bosons), or to consider specific models (which might contain, *e.g.*, Z' bosons and exotic fermions with correlated parameters). Fits to Supersymmetric models are described in Refs. 181 and 248. Models involving strong dynamics (such as (extended) Technicolor) for electroweak breaking are considered in Ref. 249. The effects of compactified extra spatial dimensions at the TeV scale are reviewed in Ref. 250, and constraints on Little Higgs models in Ref. 251. The implications of non-standard Higgs sectors, *e.g.*, involving Higgs singlets or triplets, are discussed in Ref. 252. Limits on new four-Fermi operators and on leptoquarks using LEP 2 and lower energy data are given in Refs. [160,253]. Constraints on various types of new physics are reviewed in Refs. [59,128,254,255], and implications for the LHC in Ref. 256.

An alternate formalism [257] defines parameters, ϵ_1 , ϵ_2 , ϵ_3 , and ϵ_b in terms of the specific observables M_W/M_Z , $\Gamma_{\ell\ell}$, $A_{FB}^{(0,\ell)}$, and R_b . The definitions coincide with those for $\hat{\epsilon}_i$ in Eqs. (10.55) and (10.56) for physics which affects gauge self-energies only, but the ϵ 's now parametrize arbitrary types of new physics. However, the ϵ 's are not related to other observables unless additional model-dependent assumptions are made. Another approach [258] parametrizes new physics in terms of gauge-invariant sets of operators. It is especially powerful in studying the effects of new physics on non-Abelian gauge vertices. The most general approach introduces deviation vectors [254]. Each type of new physics defines a deviation vector, the components of which are the deviations of each observable from its SM prediction, normalized to the experimental uncertainty. The length (direction) of the vector represents the strength (type) of new physics.

One of the best motivated kinds of physics beyond the SM besides Supersymmetry are extra Z' bosons [259]. They do not spoil the observed approximate gauge coupling unification, and appear copiously in many Grand Unified Theories (GUTs), most Superstring models [260], as well as in dynamical symmetry breaking [249] and Little Higgs models [251]. For example, the $SO(10)$ GUT contains an extra $U(1)$ as can be seen from its maximal subgroup, $SU(5) \times U(1)_\chi$. Similarly, the E_6 GUT contains the subgroup $SO(10) \times U(1)_\psi$. The Z_ψ possesses only axial-vector couplings to the ordinary fermions, and its mass is generally less constrained. The Z_η boson is the linear

Table 10.10: 95% CL lower mass limits (in GeV) from low energy and Z pole data on various extra Z' gauge bosons, appearing in models of unification and string theory. More general parametrizations are described in Refs. 259,264. The electroweak results [265] are for Higgs sectors consisting of doublets and singlets only ($\rho_0 = 1$) with unspecified $U(1)'$ charges. The CDF [266] and DØ [267] bounds from searches for $\bar{p}p \rightarrow \mu^+\mu^-$ and e^+e^- , respectively, are listed in the next two columns, followed by the LEP 2 $e^+e^- \rightarrow f\bar{f}$ bounds [160] (assuming $\theta = 0$). (The Tevatron bounds would be moderately weakened if there are open supersymmetric or exotic decay channels [268]) . The last column shows the 1σ ranges for M_H when it is left unconstrained in the electroweak fits.

Z'	electroweak	CDF	DØ	LEP 2	M_H
Z_χ	1, 141	892	800	673	171^{+493}_{-89}
Z_ψ	147	878	763	481	97^{+31}_{-25}
Z_η	427	982	810	434	423^{+577}_{-350}
Z_{LR}	998	630	–	804	804^{+174}_{-35}
Z_S	1, 257	821	719	–	149^{+353}_{-68}
Z_{SM}	1, 403	1, 030	950	1, 787	331^{+669}_{-246}
Z_{string}	1, 362	–	–	–	134^{+209}_{-58}

combination $\sqrt{3/8}Z_\chi - \sqrt{5/8}Z_\psi$. The Z_{LR} boson occurs in left-right models with gauge group $SU(3)_C \times SU(2)_L \times SU(2)_R \times U(1)_{B-L} \subset SO(10)$, and the secluded Z_S emerges in a supersymmetric bottom-up scenario [261]. The sequential Z_{SM} boson is defined to have the same couplings to fermions as the SM Z boson. Such a boson is not expected in the context of gauge theories unless it has different couplings to exotic fermions than the ordinary Z boson. However, it serves as a useful reference case when comparing constraints from various sources. It could also play the role of an excited state of the ordinary Z boson in models with extra dimensions at the weak scale [250]. Finally, we consider a Superstring motivated Z_{string} boson appearing in a specific model [262]. The potential Z' boson is in general a superposition of the SM Z and the new boson associated with the extra $U(1)$. The mixing angle θ satisfies,

$$\tan^2 \theta = \frac{M_{Z_1^0}^2 - M_Z^2}{M_{Z'}^2 - M_{Z_1^0}^2},$$

where $M_{Z_1^0}$ is the SM value for M_Z in the absence of mixing. Note, that $M_Z < M_{Z_1^0}$, and that the SM Z couplings are changed by the mixing. The couplings of the heavier Z' may also be modified by kinetic mixing [259,263]. If the Higgs $U(1)'$ quantum numbers

42 10. Electroweak model and constraints on new physics

are known, there will be an extra constraint,

$$\theta = C \frac{g_2}{g_1} \frac{M_Z^2}{M_{Z'}^2},$$

where $g_{1,2}$ are the U(1) and U(1)' gauge couplings with $g_2 = \sqrt{\frac{5}{3}} \sin \theta_W \sqrt{\lambda} g_1$ and $g_1 = \sqrt{g^2 + g'^2}$. $\lambda \sim 1$ (which we assume) if the GUT group breaks directly to $SU(3) \times SU(2) \times U(1) \times U(1)'$. C is a function of vacuum expectation values. For minimal Higgs sectors it can be found in Ref. 223. Table 10.10 shows the 95% CL lower mass limits [265] for $\rho_0 = 1$ and $114.4 \text{ GeV} \leq M_H \leq 1 \text{ TeV}$. The last column shows the 1σ ranges for M_H when it is left unconstrained. In cases of specific minimal Higgs sectors where C is known, the Z' mass limits are generally pushed into the TeV region. The limits on $|\theta|$ are typically smaller than a few $\times 10^{-3}$. For more details see [259,265,269] and the note on “The Z' Searches” in the Gauge & Higgs Boson Particle Listings. Also listed in Table 10.10 are the direct lower limits on Z' production from the Tevatron [266,267] and LEP 2 bounds [160].

Acknowledgments:

This work was supported in part by CONACyT (México) contract 82291–F by an IBM Einstein Fellowship, and by NSF grant PHY–0503584.

References:

1. S. Weinberg, Phys. Rev. Lett. **19**, 1264 (1967);
A. Salam, p. 367 of *Elementary Particle Theory*, ed. N. Svartholm (Almquist and Wiksells, Stockholm, 1969);
S.L. Glashow, J. Iliopoulos, and L. Maiani, Phys. Rev. **D2**, 1285 (1970).
2. CKMfitter Group: J. Charles *et al.*, Eur. Phys. J. **C41**, 1 (2005);
V. Tisserand *et al.*, 0905.1572 [hep-ph].
3. For reviews, see G. Barbiellini and C. Santoni, Riv. Nuovo Cimento **9(2)**, 1 (1986);
E.D. Commins and P.H. Bucksbaum, *Weak Interactions of Leptons and Quarks*, (Cambridge Univ. Press, 1983);
W. Fetscher and H.J. Gerber, p. 657 of Ref. 4;
J. Deutsch and P. Quin, p. 706 of Ref. 4;
J.M. Conrad, M.H. Shaevitz, and T. Bolton, Rev. Mod. Phys. **70**, 1341 (1998);
N. Severijns, M. Beck,, and O. Naviliat-Cuncic, Rev. Mod. Phys. **78**, 991 (2006);
P. Langacker, *The Standard Model and Beyond*, (CRC Press, New York, 2009).
4. *Precision Tests of the Standard Electroweak Model*, ed. P. Langacker (World Scientific, Singapore, 1995).
5. J. Erler and M. Luo, Phys. Lett. **B558**, 125 (2003).
6. Tevatron Electroweak Working Group, CDF and DØ: 0903.2503 [hep-ex].
7. K. Melnikov and T. van Ritbergen, Phys. Lett. **B482**, 99 (2000).
8. S.J. Brodsky, G.P. Lepage, and P.B. Mackenzie, Phys. Rev. **D28**, 228 (1983).
9. N. Gray *et al.*, Z. Phys. **C48**, 673 (1990).

10. For reviews, see the Section on “Higgs Bosons: Theory and Searches” in this *Review*;
 J. Gunion *et al.*, *The Higgs Hunter’s Guide*, (Addison-Wesley, Redwood City, 1990);
 M. Carena and H.E. Haber, *Prog. in Part. Nucl. Phys.* **50**, 63 (2003);
 U. Aglietti *et al.*, [hep-ph/0612172](#);
 M. Gomez-Bock *et al.*, [arXiv:0712.2419 \[hep-ph\]](#);
 A. Djouadi, *Phys. Reports* **457**, 1 (2008);
 A. Djouadi, *Phys. Reports* **459**, 1 (2008).
11. ALEPH, DELPHI, L3, OPAL, SLD, LEP Electroweak Working Group, SLD Electroweak and Heavy Flavour Groups: S. Schael *et al.*, *Phys. Reports* **427**, 257 (2006); for updates see <http://lepewwg.web.cern.ch/LEPEWWG/>.
12. D. Hanneke, S. Fogwell and G. Gabrielse, *Phys. Rev. Lett.* **100**, 120801 (2008).
13. T. Aoyama, M. Hayakawa, T. Kinoshita and M. Nio, *Phys. Rev.* **D77**, 053012 (2008).
14. P.J. Mohr, B.N. Taylor and D.B. Newell, *Rev. Mod. Phys.* **80**, 633 (2008).
15. For a review, see S. Mele, [hep-ex/0610037](#).
16. S. Fanchiotti, B. Kniehl, and A. Sirlin, *Phys. Rev.* **D48**, 307 (1993) and references therein.
17. J. Erler, *Phys. Rev.* **D59**, 054008 (1999).
18. M. Beneke, *Phys. Reports* **317**, 1 (1999).
19. A.D. Martin and D. Zeppenfeld, *Phys. Lett.* **B345**, 558 (1995).
20. S. Eidelman and F. Jegerlehner, *Z. Phys.* **C67**, 585 (1995).
21. B.V. Geshkenbein and V.L. Morgunov, *Phys. Lett.* **B340**, 185 (1995);
 B.V. Geshkenbein and V.L. Morgunov, *Phys. Lett.* **B352**, 456 (1995).
22. H. Burkhardt and B. Pietrzyk, *Phys. Lett.* **B356**, 398 (1995).
23. M.L. Swartz, *Phys. Rev.* **D53**, 5268 (1996).
24. R. Alemany, M. Davier, and A. Höcker, *Eur. Phys. J.* **C2**, 123 (1998).
25. N.V. Krasnikov and R. Rodenberg, *Nuovo Cimento* **111A**, 217 (1998).
26. M. Davier and A. Höcker, *Phys. Lett.* **B419**, 419 (1998).
27. J.H. Kühn and M. Steinhauser, *Phys. Lett.* **B437**, 425 (1998).
28. M. Davier and A. Höcker, *Phys. Lett.* **B435**, 427 (1998).
29. S. Groote *et al.*, *Phys. Lett.* **B440**, 375 (1998).
30. A.D. Martin, J. Outhwaite, and M.G. Ryskin, *Phys. Lett.* **B492**, 69 (2000).
31. H. Burkhardt and B. Pietrzyk, *Phys. Lett.* **B513**, 46 (2001).
32. J.F. de Troconiz and F.J. Yndurain, *Phys. Rev.* **D65**, 093002 (2002).
33. F. Jegerlehner, *Nucl. Phys. Proc. Suppl.* **126**, 325 (2004).
34. K. Hagiwara *et al.*, *Phys. Rev.* **D69**, 093003 (2004).
35. H. Burkhardt and B. Pietrzyk, *Phys. Rev.* **D72**, 057501 (2005).
36. K. Hagiwara *et al.*, *Phys. Lett.* **B649**, 173 (2007).
37. F. Jegerlehner, *Nucl. Phys. Proc. Suppl.* **181-182**, 135 (2008).
38. BES: J.Z. Bai *et al.*, *Phys. Rev. Lett.* **88**, 101802 (2002);
 G.S. Huang, [hep-ex/0105074](#).
39. M. Davier *et al.*, *Eur. Phys. J.* **C31**, 503 (2003).

44 10. Electroweak model and constraints on new physics

40. M. Davier *et al.*, Eur. Phys. J. **C66**, 127 (2010).
41. OPAL: K. Ackerstaff *et al.*, Eur. Phys. J. **C7**, 571 (1999).
42. CLEO: S. Anderson *et al.*, Phys. Rev. **D61**, 112002 (2000).
43. ALEPH: S. Schael *et al.*, Phys. Reports **421**, 191 (2005).
44. Belle: M. Fujikawa *et al.*: Phys. Rev. **D78**, 072006 (2008).
45. CMD-2: R.R. Akhmetshin *et al.*, Phys. Lett. **B578**, 285 (2004);
CMD-2: V.M. Aulchenko *et al.*, JETP Lett. **82**, 743 (2005);
CMD-2: R.R. Akhmetshin *et al.*, JETP Lett. **84**, 413 (2006);
CMD-2: R.R. Akhmetshin *et al.*, Phys. Lett. **B648**, 28 (2007).
46. SND: M.N. Achasov *et al.*, Sov. Phys. JETP **103**, 380 (2006).
47. A.B. Arbuzov *et al.*, JHEP **9812**, 009 (1998);
S. Binner, J.H. Kühn, and K. Melnikov, Phys. Lett. **B459**, 279 (1999).
48. BaBar: B. Aubert *et al.*, Phys. Rev. **D70**, 072004 (2004);
BaBar: B. Aubert *et al.*, Phys. Rev. **D71**, 052001 (2005);
BaBar: B. Aubert *et al.*, Phys. Rev. **D73**, 052003 (2006);
BaBar: B. Aubert *et al.*, Phys. Rev. **D76**, 092005 (2007);
BaBar: B. Aubert *et al.*, Phys. Rev. Lett. **103**, 231801 (2009).
49. KLOE: F. Ambrosino *et al.*, Phys. Lett. **B670**, 285 (2009).
50. M. Davier *et al.*, Eur. Phys. J. **C66**, 1 (2010).
51. See *e.g.*, CMD and OLYA: L.M. Barkov *et al.*, Nucl. Phys. **B256**, 365 (1985).
52. W.J. Marciano and A. Sirlin, Phys. Rev. Lett. **61**, 1815 (1988).
53. T. van Ritbergen and R.G. Stuart, Phys. Rev. Lett. **82**, 488 (1999).
54. Y. Nir, Phys. Lett. **B221**, 184 (1989).
55. A. Pak and A. Czarnecki, Phys. Rev. Lett. **100**, 241807 (2008).
56. MuLan: D.B. Chitwood *et al.*, Phys. Rev. Lett. **99**, 032001 (2007).
57. FAST: A. Barczyk *et al.*, Phys. Lett. **B663**, 172 (2008).
58. Earlier analyses include U. Amaldi *et al.*, Phys. Rev. **D36**, 1385 (1987);
G. Costa *et al.*, Nucl. Phys. **B297**, 244 (1988);
Deep inelastic scattering is considered by G.L. Fogli and D. Haidt, Z. Phys. **C40**, 379 (1988);
P. Langacker and M. Luo, Phys. Rev. **D44**, 817 (1991);
For more recent analyses, see Ref. 59.
59. P. Langacker, p. 883 of Ref. 4;
J. Erler and P. Langacker, Phys. Rev. **D52**, 441 (1995).
60. J. Erler and M.J. Ramsey-Musolf, Prog. in Part. Nucl. Phys. **54**, 351 (2005);
Neutrino scattering is reviewed by J.M. Conrad *et al.* in Ref. 3;
Nonstandard neutrino interactions are surveyed in Z. Berezhiani and A. Rossi,
Phys. Lett. **B535**, 207 (2002);
S. Davidson *et al.*, JHEP **0303**, 011 (2003);
A. Friedland, C. Lunardini and C. Pena-Garay, Phys. Lett. **B594**, 347 (2004).
61. A. Sirlin, Phys. Rev. **D22**, 971 (1980);
A. Sirlin, Phys. Rev. **D29**, 89 (1984);
D.C. Kennedy *et al.*, Nucl. Phys. **B321**, 83 (1989);
D.C. Kennedy and B.W. Lynn, Nucl. Phys. **B322**, 1 (1989);

- D.Yu. Bardin *et al.*, *Z. Phys.* **C44**, 493 (1989);
W. Hollik, *Fortsch. Phys.* **38**, 165 (1990);
For reviews, see the articles by W. Hollik, pp. 37 and 117, and W. Marciano, p. 170 in Ref. 4. Extensive references to other papers are given in Ref. 58.
62. V.A. Novikov, L.B. Okun, and M.I. Vysotsky, *Nucl. Phys.* **B397**, 35 (1993).
 63. W. Hollik in Ref. 61 and references therein.
 64. W.J. Marciano and J.L. Rosner, *Phys. Rev. Lett.* **65**, 2963 (1990).
 65. G. Degrassi, S. Fanchiotti, and A. Sirlin, *Nucl. Phys.* **B351**, 49 (1991).
 66. G. Degrassi and A. Sirlin, *Nucl. Phys.* **B352**, 342 (1991).
 67. P. Gambino and A. Sirlin, *Phys. Rev.* **D49**, 1160 (1994).
 68. ZFITTER: D. Bardin *et al.*, *Comput. Phys. Commun.* **133**, 229 (2001) and references therein;
ZFITTER: A.B. Arbuzov *et al.*, *Comput. Phys. Commun.* **174**, 728 (2006).
 69. R. Barbieri *et al.*, *Phys. Lett.* **B288**, 95 (1992) and *ibid.*, **312**, 511(E) (1993);
R. Barbieri *et al.*, *Nucl. Phys.* **B409**, 105 (1993).
 70. J. Fleischer, O.V. Tarasov, and F. Jegerlehner, *Phys. Lett.* **B319**, 249 (1993).
 71. G. Degrassi, P. Gambino, and A. Vicini, *Phys. Lett.* **B383**, 219 (1996);
G. Degrassi, P. Gambino, and A. Sirlin, *Phys. Lett.* **B394**, 188 (1997).
 72. A. Freitas *et al.*, *Phys. Lett.* **B495**, 338 (2000) and *ibid.*, **570**, 260(E) (2003);
M. Awramik and M. Czakon, *Phys. Lett.* **B568**, 48 (2003).
 73. A. Freitas *et al.*, *Nucl. Phys.* **B632**, 189 (2002) and *ibid.*, **666**, 305(E) (2003);
M. Awramik and M. Czakon, *Phys. Rev. Lett.* **89**, 241801 (2002);
A. Onishchenko and O. Veretin, *Phys. Lett.* **B551**, 111 (2003).
 74. M. Awramik *et al.*, *Phys. Rev. Lett.* **93**, 201805 (2004);
W. Hollik, U. Meier, and S. Uccirati, *Nucl. Phys.* **B731**, 213 (2005).
 75. M. Awramik, M. Czakon, and A. Freitas, *Phys. Lett.* **B642**, 563 (2006);
M. Awramik, M. Czakon and A. Freitas, *JHEP* **0611**, 048 (2006);
W. Hollik, U. Meier, and S. Uccirati, *Nucl. Phys.* **B765**, 154 (2007).
 76. A. Djouadi and C. Verzegnassi, *Phys. Lett.* **B195**, 265 (1987);
A. Djouadi, *Nuovo Cimento* **100A**, 357 (1988).
 77. K.G. Chetyrkin, J.H. Kühn, and M. Steinhauser, *Phys. Lett.* **B351**, 331 (1995);
L. Avdeev *et al.*, *Phys. Lett.* **B336**, 560 (1994) and *ibid.*, **B349**, 597(E) (1995).
 78. B.A. Kniehl, J.H. Kühn, and R.G. Stuart, *Phys. Lett.* **B214**, 621 (1988);
B.A. Kniehl, *Nucl. Phys.* **B347**, 86 (1990);
F. Halzen and B.A. Kniehl, *Nucl. Phys.* **B353**, 567 (1991);
A. Djouadi and P. Gambino, *Phys. Rev.* **D49**, 4705 (1994);
A. Djouadi and P. Gambino, *Phys. Rev.* **D49**, 3499 (1994) and *ibid.*, **53**, 4111(E) (1996).
 79. K.G. Chetyrkin, J.H. Kühn, and M. Steinhauser, *Phys. Rev. Lett.* **75**, 3394 (1995).
 80. J.J. van der Bij *et al.*, *Phys. Lett.* **B498**, 156 (2001).
 81. M. Faisst *et al.*, *Nucl. Phys.* **B665**, 649 (2003).
 82. R. Boughezal, J.B. Tausk, and J.J. van der Bij, *Nucl. Phys.* **B713**, 278 (2005);
R. Boughezal, J.B. Tausk, and J.J. van der Bij, *Nucl. Phys.* **B725**, 3 (2005).
 83. A. Anselm, N. Dombey, and E. Leader, *Phys. Lett.* **B312**, 232 (1993).

46 10. Electroweak model and constraints on new physics

84. Y. Schröder and M. Steinhauser, Phys. Lett. **B622**, 124 (2005).
85. K.G. Chetyrkin *et al.*, Phys. Rev. Lett. **97**, 102003 (2006);
R. Boughezal and M. Czakon, Nucl. Phys. **B755**, 221 (2006).
86. J. Fleischer *et al.*, Phys. Lett. **B293**, 437 (1992);
K.G. Chetyrkin, A. Kwiatkowski, and M. Steinhauser, Mod. Phys. Lett. **A8**, 2785 (1993).
87. R. Harlander, T. Seidensticker, and M. Steinhauser, Phys. Lett. **B426**, 125 (1998);
J. Fleischer *et al.*, Phys. Lett. **B459**, 625 (1999).
88. M. Awramik, M. Czakon, A. Freitas and B. A. Kniehl, Nucl. Phys. **B813**, 174 (2009).
89. A. Czarnecki and J.H. Kühn, Phys. Rev. Lett. **77**, 3955 (1996).
90. J. Erler, hep-ph/0005084.
91. For reviews, see F. Perrier, p. 385 of Ref. 4;
J.M. Conrad *et al.* in Ref. 3.
92. CDHS: H. Abramowicz *et al.*, Phys. Rev. Lett. **57**, 298 (1986);
CDHS: A. Blondel *et al.*, Z. Phys. **C45**, 361 (1990).
93. CHARM: J.V. Allaby *et al.*, Phys. Lett. **B177**, 446 (1986);
CHARM: J.V. Allaby *et al.*, Z. Phys. **C36**, 611 (1987).
94. CCFR: C.G. Arroyo *et al.*, Phys. Rev. Lett. **72**, 3452 (1994);
CCFR: K.S. McFarland *et al.*, Eur. Phys. J. **C1**, 509 (1998).
95. R.M. Barnett, Phys. Rev. **D14**, 70 (1976);
H. Georgi and H.D. Politzer, Phys. Rev. **D14**, 1829 (1976).
96. LAB-E: S.A. Rabinowitz *et al.*, Phys. Rev. Lett. **70**, 134 (1993).
97. E.A. Paschos and L. Wolfenstein, Phys. Rev. **D7**, 91 (1973).
98. NuTeV: G.P. Zeller *et al.*, Phys. Rev. Lett. **88**, 091802 (2002).
99. D. Mason *et al.*, Phys. Rev. Lett. **99**, 192001 (2007).
100. S. Kretzer, D. Mason, and F. Olness, Phys. Rev. **D65**, 074010 (2002).
101. J. Pumplin *et al.*, JHEP **0207**, 012 (2002);
S. Kretzer *et al.*, Phys. Rev. Lett. **93**, 041802 (2004).
102. NuTeV: G.P. Zeller *et al.*, Phys. Rev. **D65**, 111103 (2002) and *ibid.*, **D67**, 119902(E) (2003).
103. W. Bentz *et al.*, arXiv:0908.3198 [nucl-th];
for further reviews including discussions of possible new physics explanations, see
S. Davidson *et al.*, JHEP **0202**, 037 (2002);
J.T. Londergan, Eur. Phys. J. **A32**, 415 (2007).
104. E. Sather, Phys. Lett. **B274**, 433 (1992);
E.N. Rodionov, A.W. Thomas, and J.T. Londergan, Mod. Phys. Lett. **A9**, 1799 (1994).
105. A.D. Martin *et al.*, Eur. Phys. J. **C35**, 325 (2004).
106. A.D. Martin *et al.*, Eur. Phys. J. **C39**, 155 (2005).
107. J.T. Londergan and A.W. Thomas, Phys. Rev. **D67**, 111901 (2003).
108. M. Glück, P. Jimenez-Delgado and E. Reya, Phys. Rev. Lett. **95**, 022002 (2005).
109. S. Kumano, Phys. Rev. **D66**, 111301 (2002);
S.A. Kulagin, Phys. Rev. **D67**, 091301 (2003);

- S.J. Brodsky, I. Schmidt, and J.J. Yang, Phys. Rev. **D70**, 116003 (2004);
M. Hirai, S. Kumano, and T. H. Nagai, Phys. Rev. **D71**, 113007 (2005);
G.A. Miller and A.W. Thomas, Int. J. Mod. Phys. A **20**, 95 (2005).
110. I.C. Cloet, W. Bentz and A.W. Thomas, Phys. Rev. Lett. **102**, 252301 (2009).
111. K.P.O. Diener, S. Dittmaier, and W. Hollik, Phys. Rev. **D69**, 073005 (2004);
A.B. Arbuzov, D.Y. Bardin, and L.V. Kalinovskaya, JHEP **0506**, 078 (2005);
K. Park, U. Baur and D. Wackerath, arXiv:0910.5013 [hep-ph].
112. K.P.O. Diener, S. Dittmaier, and W. Hollik, Phys. Rev. **D72**, 093002 (2005).
113. B.A. Dobrescu and R.K. Ellis, Phys. Rev. **D69**, 114014 (2004).
114. CHARM: J. Dorenbosch *et al.*, Z. Phys. **C41**, 567 (1989).
115. CALO: L.A. Ahrens *et al.*, Phys. Rev. **D41**, 3297 (1990).
116. CHARM II: P. Vilain *et al.*, Phys. Lett. **B335**, 246 (1994).
117. For a review, see J. Panman, p. 504 of Ref. 4.
118. ILM: R.C. Allen *et al.*, Phys. Rev. **D47**, 11 (1993);
LSND: L.B. Auerbach *et al.*, Phys. Rev. **D63**, 112001 (2001).
119. SSF: C.Y. Prescott *et al.*, Phys. Lett. **B84**, 524 (1979).
120. E.J. Beise, M.L. Pitt and D.T. Spayde, Prog. in Part. Nucl. Phys. **54**, 289 (2005).
121. S.L. Zhu *et al.*, Phys. Rev. **D62**, 033008 (2000).
122. P. Souder, p. 599 of Ref. 4.
123. R.D. Young *et al.*, Phys. Rev. Lett. **99**, 122003 (2007).
124. E. Derman and W.J. Marciano, Annals Phys. **121**, 147 (1979).
125. E158: P.L. Anthony *et al.*, Phys. Rev. Lett. **95**, 081601 (2005).
126. A. Czarnecki and W.J. Marciano, Int. J. Mod. Phys. A **15**, 2365 (2000).
127. Qweak: M.T. Gericke *et al.*, AIP Conf. Proc. **1149**, 237 (2009);
the implications are discussed in Ref. 128.
128. J. Erler, A. Kurylov, and M.J. Ramsey-Musolf, Phys. Rev. **D68**, 016006 (2003).
129. J. Erler and M.J. Ramsey-Musolf, Phys. Rev. **D72**, 073003 (2005).
130. C. Bouchiat and C.A. Piketty, Phys. Lett. **B128**, 73 (1983).
131. For reviews and references to earlier work, see M.A. Bouchiat and L. Pottier,
Science **234**, 1203 (1986);
B.P. Masterson and C.E. Wieman, p. 545 of Ref. 4.
132. Cesium (Boulder): C.S. Wood *et al.*, Science **275**, 1759 (1997).
133. Cesium (Paris): J. Guéna, M. Lintz, and M.A. Bouchiat, Phys. Rev. **A71**, 042108
(2005).
134. Thallium (Oxford): N.H. Edwards *et al.*, Phys. Rev. Lett. **74**, 2654 (1995);
Thallium (Seattle): P.A. Vetter *et al.*, Phys. Rev. Lett. **74**, 2658 (1995).
135. Lead (Seattle): D.M. Meekhof *et al.*, Phys. Rev. Lett. **71**, 3442 (1993).
136. Bismuth (Oxford): M.J.D. MacPherson *et al.*, Phys. Rev. Lett. **67**, 2784 (1991).
137. V.A. Dzuba, V.V. Flambaum, and O.P. Sushkov, Phys. Lett. **141A**, 147 (1989);
S.A. Blundell, J. Sapirstein, and W.R. Johnson, Phys. Rev. Lett. **65**, 1411 (1990);
S.A. Blundell, J. Sapirstein, and W.R. Johnson, Phys. Rev. **D45**, 1602 (1992);
For reviews, see S.A. Blundell, W.R. Johnson, and J. Sapirstein, p. 577 of Ref. 4;
J.S.M. Ginges and V.V. Flambaum, Phys. Reports **397**, 63 (2004);

48 10. Electroweak model and constraints on new physics

- J. Guena, M. Lintz, and M. A. Bouchiat, *Mod. Phys. Lett.* **A20**, 375 (2005);
A. Derevianko and S.G. Porsev, *Eur. Phys. J. A* **32**, 517 (2007).
138. V.A. Dzuba, V.V. Flambaum, and O.P. Sushkov, *Phys. Rev.* **A56**, R4357 (1997).
139. S.C. Bennett and C.E. Wieman, *Phys. Rev. Lett.* **82**, 2484 (1999).
140. M.A. Bouchiat and J. Guéna, *J. Phys. (France)* **49**, 2037 (1988).
141. S. G. Porsev, K. Beloy and A. Derevianko, *Phys. Rev. Lett.* **102**, 181601 (2009).
142. A. Derevianko, *Phys. Rev. Lett.* **85**, 1618 (2000);
V.A. Dzuba, C. Harabati, and W.R. Johnson, *Phys. Rev.* **A63**, 044103 (2001);
M.G. Kozlov, S.G. Porsev, and I.I. Tupitsyn, *Phys. Rev. Lett.* **86**, 3260 (2001);
W.R. Johnson, I. Bednyakov, and G. Soff, *Phys. Rev. Lett.* **87**, 233001 (2001);
A.I. Milstein and O.P. Sushkov, *Phys. Rev.* **A66**, 022108 (2002);
V.A. Dzuba, V.V. Flambaum, and J.S. Ginges, *Phys. Rev.* **D66**, 076013 (2002);
M.Y. Kuchiev and V.V. Flambaum, *Phys. Rev. Lett.* **89**, 283002 (2002);
A.I. Milstein, O.P. Sushkov, and I.S. Terekhov, *Phys. Rev. Lett.* **89**, 283003 (2002);
V.V. Flambaum and J.S.M. Ginges, *Phys. Rev.* **A72**, 052115 (2005).
143. V.A. Dzuba *et al.*, *J. Phys.* **B20**, 3297 (1987).
144. Ya.B. Zel'dovich, *Sov. Phys. JETP* **6**, 1184 (1958);
For recent discussions, see V.V. Flambaum and D.W. Murray, *Phys. Rev.* **C56**, 1641 (1997);
W.C. Haxton and C.E. Wieman, *Ann. Rev. Nucl. Part. Sci.* **51**, 261 (2001).
145. J.L. Rosner, *Phys. Rev.* **D53**, 2724 (1996).
146. S.J. Pollock, E.N. Fortson, and L. Willets, *Phys. Rev.* **C46**, 2587 (1992);
B.Q. Chen and P. Vogel, *Phys. Rev.* **C48**, 1392 (1993).
147. R.W. Dunford and R.J. Holt, *J. Phys.* **G34**, 2099 (2007).
148. B.W. Lynn and R.G. Stuart, *Nucl. Phys.* **B253**, 216 (1985).
149. *Physics at LEP*, ed. J. Ellis and R. Peccei, CERN 86-02, Vol. 1.
150. PETRA: S.L. Wu, *Phys. Reports* **107**, 59 (1984);
C. Kiesling, *Tests of the Standard Theory of Electroweak Interactions*, (Springer-Verlag, New York, 1988);
R. Marshall, *Z. Phys.* **C43**, 607 (1989);
Y. Mori *et al.*, *Phys. Lett.* **B218**, 499 (1989);
D. Haidt, p. 203 of Ref. 4.
151. For reviews, see D. Schaile, p. 215, and A. Blondel, p. 277 of Ref. 4.
152. SLD: K. Abe *et al.*, *Phys. Rev. Lett.* **84**, 5945 (2000).
153. SLD: K. Abe *et al.*, *Phys. Rev. Lett.* **85**, 5059 (2000).
154. SLD: K. Abe *et al.*, *Phys. Rev. Lett.* **86**, 1162 (2001).
155. DELPHI: P. Abreu *et al.*, *Z. Phys.* **C67**, 1 (1995);
OPAL: K. Ackerstaff *et al.*, *Z. Phys.* **C76**, 387 (1997).
156. SLD: K. Abe *et al.*, *Phys. Rev. Lett.* **78**, 17 (1997).
157. CDF: D. Acosta *et al.*, *Phys. Rev.* **D71**, 052002 (2005).
158. DØ: V.M. Abazov *et al.*, *Phys. Rev. Lett.* **101**, 191801 (2008).
159. H1: A. Aktas *et al.*, *Phys. Lett.* **B632**, 35 (2006);
H1 and ZEUS: Z. Zhang, *Nucl. Phys. Proc. Suppl.* **191**, 271 (2009).

160. ALEPH, DELPHI, L3, OPAL, and LEP Electroweak Working Group: J. Alcarez *et al.*, hep-ex/0612034.
161. ALEPH, DELPHI, L3, OPAL, and the LEP Working Group for Higgs Boson Searches: D. Abbaneo *et al.*, Phys. Lett. **B565**, 61 (2003).
162. J. Erler, Phys. Rev. **D81**, 051301 (R) (2010).
163. A. Leike, T. Riemann, and J. Rose, Phys. Lett. **B273**, 513 (1991);
T. Riemann, Phys. Lett. **B293**, 451 (1992).
164. A comprehensive report and further references can be found in K.G. Chetyrkin, J.H. Kühn, and A. Kwiatkowski, Phys. Reports **277**, 189 (1996).
165. J. Schwinger, *Particles, Sources, and Fields*, Vol. II, (Addison-Wesley, New York, 1973);
K.G. Chetyrkin, A.L. Kataev, and F.V. Tkachev, Phys. Lett. **B85**, 277 (1979);
M. Dine and J. Sapirstein, Phys. Rev. Lett. **43**, 668 (1979);
W. Celmaster and R.J. Gonsalves, Phys. Rev. Lett. **44**, 560 (1980);
S.G. Gorishnii, A.L. Kataev, and S.A. Larin, Phys. Lett. **B212**, 238 (1988);
S.G. Gorishnii, A.L. Kataev, and S.A. Larin, Phys. Lett. **B259**, 144 (1991);
L.R. Surguladze and M.A. Samuel, Phys. Rev. Lett. **66**, 560 (1991) and *ibid.*, 2416(E).
166. P.A. Baikov, K.G. Chetyrkin, and J.H. Kühn, Phys. Rev. Lett. **101**, 012002 (2008).
167. W. Bernreuther and W. Wetzel, Z. Phys. **11**, 113 (1981);
W. Bernreuther and W. Wetzel, Phys. Rev. **D24**, 2724 (1982);
B.A. Kniehl, Phys. Lett. **B237**, 127 (1990);
K.G. Chetyrkin, Phys. Lett. **B307**, 169 (1993);
A.H. Hoang *et al.*, Phys. Lett. **B338**, 330 (1994);
S.A. Larin, T. van Ritbergen, and J.A.M. Vermaseren, Nucl. Phys. **B438**, 278 (1995).
168. T.H. Chang, K.J.F. Gaemers, and W.L. van Neerven, Nucl. Phys. **B202**, 407 (1980);
J. Jersak, E. Laermann, and P.M. Zerwas, Phys. Lett. **B98**, 363 (1981);
J. Jersak, E. Laermann, and P.M. Zerwas, Phys. Rev. **D25**, 1218 (1982);
S.G. Gorishnii, A.L. Kataev, and S.A. Larin, Nuovo Cimento **92**, 117 (1986);
K.G. Chetyrkin and J.H. Kühn, Phys. Lett. **B248**, 359 (1990);
K.G. Chetyrkin, J.H. Kühn, and A. Kwiatkowski, Phys. Lett. **B282**, 221 (1992);
K.G. Chetyrkin and J.H. Kühn, Phys. Lett. **B406**, 102 (1997).
169. B.A. Kniehl and J.H. Kühn, Phys. Lett. **B224**, 229 (1990);
B.A. Kniehl and J.H. Kühn, Nucl. Phys. **B329**, 547 (1990);
K.G. Chetyrkin and A. Kwiatkowski, Phys. Lett. **B305**, 285 (1993);
K.G. Chetyrkin and A. Kwiatkowski, Phys. Lett. **B319**, 307 (1993);
S.A. Larin, T. van Ritbergen, and J.A.M. Vermaseren, Phys. Lett. **B320**, 159 (1994);
K.G. Chetyrkin and O.V. Tarasov, Phys. Lett. **B327**, 114 (1994).
170. A.L. Kataev, Phys. Lett. **B287**, 209 (1992).
171. D. Albert *et al.*, Nucl. Phys. **B166**, 460 (1980);
F. Jegerlehner, Z. Phys. **C32**, 425 (1986);

50 10. Electroweak model and constraints on new physics

- A. Djouadi, J.H. Kühn, and P.M. Zerwas, *Z. Phys.* **C46**, 411 (1990);
A. Borrelli *et al.*, *Nucl. Phys.* **B333**, 357 (1990).
172. A.A. Akhundov, D.Yu. Bardin, and T. Riemann, *Nucl. Phys.* **B276**, 1 (1986);
W. Beenakker and W. Hollik, *Z. Phys.* **C40**, 141 (1988);
B.W. Lynn and R.G. Stuart, *Phys. Lett.* **B352**, 676 (1990);
J. Bernabeu, A. Pich, and A. Santamaria, *Nucl. Phys.* **B363**, 326 (1991).
173. Tevatron Electroweak Working Group, CDF and DØ: 1003.2826 [[hep-ex](#)].
174. CLEO: S. Chen *et al.*, *Phys. Rev. Lett.* **87**, 251807 (2001).
175. BaBar: B. Aubert *et al.*, *Phys. Rev.* **D72**, 052004 (2005);
BaBar: B. Aubert *et al.*, *Phys. Rev.* **D73**, 012005 (2006).
176. Belle: A. Limosani *et al.*, *Phys. Rev. Lett.* **103**, 241801 (2009).
177. A.L. Kagan and M. Neubert, *Eur. Phys. J.* **C7**, 5 (1999).
178. A. Ali and C. Greub, *Phys. Lett.* **B259**, 182 (1991).
179. I. Bigi and N. Uraltsev, *Int. J. Mod. Phys. A* **17**, 4709 (2002).
180. A. Czarnecki and W.J. Marciano, *Phys. Rev. Lett.* **81**, 277 (1998).
181. J. Erler and D.M. Pierce, *Nucl. Phys.* **B526**, 53 (1998).
182. K. Adel and Y.P. Yao, *Phys. Rev.* **D49**, 4945 (1994);
C. Greub, T. Hurth, and D. Wyler, *Phys. Rev.* **D54**, 3350 (1996);
K.G. Chetyrkin, M. Misiak, and M. Münz, *Phys. Lett.* **B400**, 206 (1997);
C. Greub and T. Hurth, *Phys. Rev.* **D56**, 2934 (1997);
M. Ciuchini *et al.*, *Nucl. Phys.* **B527**, 21 (1998);
M. Ciuchini *et al.*, *Nucl. Phys.* **B534**, 3 (1998);
F.M. Borzumati and C. Greub, *Phys. Rev.* **D58**, 074004 (1998);
F.M. Borzumati and C. Greub, *Phys. Rev.* **D59**, 057501 (1999);
A. Strumia, *Nucl. Phys.* **B532**, 28 (1998).
183. M. Misiak *et al.*, *Phys. Rev. Lett.* **98**, 022002 (2007).
184. F. Le Diberder and A. Pich, *Phys. Lett.* **B286**, 147 (1992).
185. M. Beneke and M. Jamin, *JHEP* **0809**, 044 (2008).
186. E. Braaten and C.S. Li, *Phys. Rev.* **D42**, 3888 (1990).
187. J. Erler, *Rev. Mex. Fis.* **50**, 200 (2004).
188. K. Maltman and T. Yavin, *Phys. Rev.* **D78**, 094020 (2008).
189. E821: G.W. Bennett *et al.*, *Phys. Rev. Lett.* **92**, 161802 (2004).
190. T. Kinoshita and M. Nio, *Phys. Rev.* **D70**, 113001 (2004);
M. Passera, *J. Phys.* **G31**, R75 (2005);
T. Kinoshita, *Nucl. Phys. Proc. Suppl.* **144**, 206 (2005).
191. G. Li, R. Mendel, and M.A. Samuel, *Phys. Rev.* **D47**, 1723 (1993);
S. Laporta and E. Remiddi, *Phys. Lett.* **B301**, 440 (1993);
S. Laporta and E. Remiddi, *Phys. Lett.* **B379**, 283 (1996);
A. Czarnecki and M. Skrzypek, *Phys. Lett.* **B449**, 354 (1999).
192. J. Erler and M. Luo, *Phys. Rev. Lett.* **87**, 071804 (2001).
193. A.L. Kataev, *Nucl. Phys. Proc. Suppl.* **155**, 369 (2006);
T. Kinoshita and M. Nio, *Phys. Rev.* **D73**, 053007 (2006).
194. For reviews, see V.W. Hughes and T. Kinoshita, *Rev. Mod. Phys.* **71**, S133 (1999);
A. Czarnecki and W.J. Marciano, *Phys. Rev.* **D64**, 013014 (2001);

- T. Kinoshita, *J. Phys.* **G29**, 9 (2003);
M. Davier and W.J. Marciano, *Ann. Rev. Nucl. Part. Sci.* **54**, 115 (2004);
J.P. Miller, E. de Rafael, and B.L. Roberts, *Rept. Prog. Phys.* **70**, 795 (2007);
F. Jegerlehner, *Acta Phys. Polon.* **B38**, 3021 (2007).
195. S.J. Brodsky and J.D. Sullivan, *Phys. Rev.* **D156**, 1644 (1967);
T. Burnett and M.J. Levine, *Phys. Lett.* **B24**, 467 (1967);
R. Jackiw and S. Weinberg, *Phys. Rev.* **D5**, 2473 (1972);
I. Bars and M. Yoshimura, *Phys. Rev.* **D6**, 374 (1972);
K. Fujikawa, B.W. Lee, and A.I. Sanda, *Phys. Rev.* **D6**, 2923 (1972);
G. Altarelli, N. Cabibbo, and L. Maiani, *Phys. Lett.* **B40**, 415 (1972);
W.A. Bardeen, R. Gastmans, and B.E. Laurup, *Nucl. Phys.* **B46**, 315 (1972).
196. T.V. Kukhto *et al.*, *Nucl. Phys.* **B371**, 567 (1992);
S. Peris, M. Perrottet, and E. de Rafael, *Phys. Lett.* **B355**, 523 (1995);
A. Czarnecki, B. Krause, and W.J. Marciano, *Phys. Rev.* **D52**, 2619 (1995);
A. Czarnecki, B. Krause, and W.J. Marciano, *Phys. Rev. Lett.* **76**, 3267 (1996).
197. G. Degrossi and G. Giudice, *Phys. Rev.* **D58**, 053007 (1998).
198. V. Cirigliano, G. Ecker, and H. Neufeld, *JHEP* **0208**, 002 (2002);
K. Maltman and C.E. Wolfe, *Phys. Rev.* **D73**, 013004 (2006).
199. S. Ghozzi and F. Jegerlehner, *Phys. Lett.* **B583**, 222 (2004).
200. K. Melnikov and A. Vainshtein, *Phys. Rev.* **D70**, 113006 (2004).
201. J. Erler and G. Toledo Sánchez, *Phys. Rev. Lett.* **97**, 161801 (2006).
202. M. Knecht and A. Nyffeler, *Phys. Rev.* **D65**, 073034 (2002).
203. M. Hayakawa and T. Kinoshita, [hep-ph/0112102](#);
J. Bijnens, E. Pallante, and J. Prades, *Nucl. Phys.* **B626**, 410 (2002);
A recent discussion is in J. Bijnens and J. Prades, *Mod. Phys. Lett.* **A22**, 767 (2007).
204. J. Prades, E. de Rafael and A. Vainshtein, 0901.0306 [[hep-ph](#)].
205. B. Krause, *Phys. Lett.* **B390**, 392 (1997).
206. J.L. Lopez, D.V. Nanopoulos, and X. Wang, *Phys. Rev.* **D49**, 366 (1994);
for recent reviews, see Ref. 194.
207. CDF: T. Affolder *et al.*, *Phys. Rev.* **D64**, 052001 (2001);
DØ: V.M. Abazov *et al.*, *Phys. Rev.* **D66**, 012001 (2002);
CDF II: T. Aaltonen *et al.*, *Phys. Rev.* **D77**, 112001 (2008);
DØ II: V.M. Abazov *et al.*, *Phys. Rev. Lett.* **103**, 141801 (2009);
Tevatron Electroweak Working Group, CDF and DØ: 0908.1374 [[hep-ex](#)].
208. F. James and M. Roos, *Comput. Phys. Commun.* **10**, 343 (1975).
209. J. Erler, J.L. Feng, and N. Polonsky, *Phys. Rev. Lett.* **78**, 3063 (1997).
210. D. Choudhury, T.M.P. Tait, and C.E.M. Wagner, *Phys. Rev.* **D65**, 053002 (2002).
211. For a recent study, see J. Cao and J.M. Yang, *JHEP* **0812**, 006 (2008).
212. J. Erler and P. Langacker, *Phys. Rev. Lett.* **84**, 212 (2000).
213. P. Langacker and M. Plümacher, *Phys. Rev.* **D62**, 013006 (2000).
214. DELPHI: P. Abreu *et al.*, *Eur. Phys. J.* **C10**, 415 (1999).
215. S. Bethke, *Phys. Reports* **403**, 203 (2004).
216. H1 and ZEUS: C. Glasman *et al.*, *J. Phys. Conf. Ser.* **110**, 022013 (2008).

217. C.T.H. Davies *et al.*, Phys. Rev. **D78**, 114507 (2008).
218. P. Langacker and N. Polonsky, Phys. Rev. **D52**, 3081 (1995);
J. Bagger, K.T. Matchev, and D. Pierce, Phys. Lett. **B348**, 443 (1995).
219. CDF and DØ: arXiv:0903.4001 [hep-ex].
220. J. Erler, Phys. Rev. **D63**, 071301 (2001).
221. CDF and DØ: T. Aaltonen *et al.*, Phys. Rev. Lett. **104**, 061802 (2010).
222. M. Veltman, Nucl. Phys. **B123**, 89 (1977);
M. Chanowitz, M.A. Furman, and I. Hinchliffe, Phys. Lett. **B78**, 285 (1978);
The two-loop correction has been obtained by J.J. van der Bij and F. Hoogeveen,
Nucl. Phys. **B283**, 477 (1987).
223. P. Langacker and M. Luo, Phys. Rev. **D45**, 278 (1992) and refs. therein.
224. A. Denner, R.J. Guth, and J.H. Kühn, Phys. Lett. **B240**, 438 (1990);
W. Grimus *et al.*, J. Phys. G **35**, 075001 (2008).
225. S. Bertolini and A. Sirlin, Phys. Lett. **B257**, 179 (1991).
226. M. Peskin and T. Takeuchi, Phys. Rev. Lett. **65**, 964 (1990);
M. Peskin and T. Takeuchi, Phys. Rev. **D46**, 381 (1992);
M. Golden and L. Randall, Nucl. Phys. **B361**, 3 (1991).
227. D. Kennedy and P. Langacker, Phys. Rev. Lett. **65**, 2967 (1990);
D. Kennedy and P. Langacker, Phys. Rev. **D44**, 1591 (1991).
228. G. Altarelli and R. Barbieri, Phys. Lett. **B253**, 161 (1990).
229. B. Holdom and J. Terning, Phys. Lett. **B247**, 88 (1990).
230. B.W. Lynn, M.E. Peskin, and R.G. Stuart, p. 90 of Ref. 149.
231. An alternative formulation is given by K. Hagiwara *et al.*, Z. Phys. **C64**, 559 (1994), and *ibid.*, **68**, 352(E) (1995);
K. Hagiwara, D. Haidt, and S. Matsumoto, Eur. Phys. J. **C2**, 95 (1998).
232. I. Maksymyk, C.P. Burgess, and D. London, Phys. Rev. **D50**, 529 (1994);
C.P. Burgess *et al.*, Phys. Lett. **B326**, 276 (1994).
233. R. Barbieri *et al.*, Nucl. Phys. **B703**, 127 (2004).
234. K. Lane, hep-ph/0202255.
235. E. Gates and J. Terning, Phys. Rev. Lett. **67**, 1840 (1991);
R. Sundrum and S.D.H. Hsu, Nucl. Phys. **B391**, 127 (1993);
R. Sundrum, Nucl. Phys. **B395**, 60 (1993);
M. Luty and R. Sundrum, Phys. Rev. Lett. **70**, 529 (1993);
T. Appelquist and J. Terning, Phys. Lett. **B315**, 139 (1993);
D.D. Dietrich, F. Sannino, and K. Tuominen, Phys. Rev. **D72**, 055001 (2005);
N.D. Christensen and R. Shrock, Phys. Lett. **B632**, 92 (2006);
M. Harada, M. Kurachi, and K. Yamawaki, Prog. Theor. Phys. **115**, 765 (2006).
236. H. Georgi, Nucl. Phys. **B363**, 301 (1991);
M.J. Dugan and L. Randall, Phys. Lett. **B264**, 154 (1991).
237. R. Barbieri *et al.*, Nucl. Phys. **B341**, 309 (1990).
238. M.E. Peskin and J.D. Wells, Phys. Rev. **D64**, 093003 (2001).
239. G.D. Kribs *et al.*, Phys. Rev. **D76**, 075016 (2007).

240. H.J. He, N. Polonsky, and S. Su, Phys. Rev. **D64**, 053004 (2001);
 V.A. Novikov *et al.*, Sov. Phys. JETP **76**, 127 (2002);
 S.S. Bulanov *et al.*, Yad. Fiz. **66**, 2219 (2003) and refs. therein.
241. J. Maalampi and M. Roos, Phys. Reports **186**, 53 (1990).
242. J. Erler and P. Langacker, arXiv:1003.3211 [hep-ph].
243. Z. Murdock, S. Nandi and Z. Tavartkiladze, Phys. Lett. **B668**, 303 (2008).
244. For reviews, see the Section on “Grand Unified Theories” in this *Review*;
 P. Langacker, Phys. Reports **72**, 185 (1981);
 J.L. Hewett and T.G. Rizzo, Phys. Reports **183**, 193 (1989);
 for collider implications, see T.C. Andre and J.L. Rosner, Phys. Rev. **D69**, 035009
 (2004);
 J. Kang, P. Langacker and B.D. Nelson, Phys. Rev. **D77**, 035003 (2008).
245. S.P. Martin, Phys. Rev. **D81**, 035004 (2010);
 P.W. Graham *et al.*, Phys. Rev. **D81**, 055016 (2010).
246. P. Langacker and D. London, Phys. Rev. **D38**, 886 (1988);
 D. London, p. 951 of Ref. 4;
 a recent analysis is F. del Aguila, J. de Blas and M. Perez-Victoria, Phys. Rev.
D78, 013010 (2008).
247. M. Chemtob, Prog. in Part. Nucl. Phys. **54**, 71 (2005);
 R. Barbier *et al.*, Phys. Reports **420**, 1 (2005).
248. G.C. Cho and K. Hagiwara, Nucl. Phys. **B574**, 623 (2000);
 G. Altarelli *et al.*, JHEP **0106**, 018 (2001);
 S. Heinemeyer, W. Hollik, and G. Weiglein, Phys. Reports **425**, 265 (2006);
 S.P. Martin, K. Tobe, and J.D. Wells, Phys. Rev. **D71**, 073014 (2005);
 G. Marandella, C. Schappacher, and A. Strumia, Nucl. Phys. **B715**, 173 (2005);
 S. Heinemeyer *et al.*, JHEP **0608**, 052 (2006);
 M.J. Ramsey-Musolf and S. Su, Phys. Reports **456**, 1 (2008);
 J.R. Ellis *et al.*, JHEP **0708**, 083 (2007);
 S. Heinemeyer *et al.*, JHEP **0804**, 039 (2008).
249. R.S. Chivukula and E.H. Simmons, Phys. Rev. **D66**, 015006 (2002);
 C.T. Hill and E.H. Simmons, Phys. Reports **381**, 235 (2003);
 R.S. Chivukula *et al.*, Phys. Rev. **D70**, 075008 (2004).
250. K. Agashe *et al.*, JHEP **0308**, 050 (2003);
 M. Carena *et al.*, Phys. Rev. **D68**, 035010 (2003);
 I. Gogoladze and C. Macesanu, Phys. Rev. **D74**, 093012 (2006);
 I. Antoniadis, hep-th/0102202 see also the note on “Extra Dimensions” in the
 Searches Particle Listings.
251. T. Han, H.E. Logan, and L.T. Wang, JHEP **0601**, 099 (2006);
 M. Perelstein, Prog. in Part. Nucl. Phys. **58**, 247 (2007).
252. E. Accomando *et al.*, arXiv:hep-ph/0608079;
 V. Barger *et al.*, Phys. Rev. **D77**, 035005 (2008);
 W. Grimus, L. Lavoura, O.M. Ogreid and P. Osland, Nucl. Phys. **B801**, 81 (2008);
 M. Maniatis, arXiv:0906.0777 [hep-ph];

54 10. Electroweak model and constraints on new physics

- U. Ellwanger, C. Hugonie and A.M. Teixeira, [arXiv:0910.1785 \[hep-ph\]](#);
M.C. Chen, S. Dawson and C.B. Jackson, *Phys. Rev.* **D78**, 093001 (2008).
253. G.C. Cho, K. Hagiwara and S. Matsumoto, *Eur. Phys. J.* **C5**, 155 (1998);
K. Cheung, *Phys. Lett.* **B517**, 167 (2001);
Z. Han and W. Skiba, *Phys. Rev.* **D71**, 075009 (2005).
254. P. Langacker, M. Luo, and A.K. Mann, *Rev. Mod. Phys.* **64**, 87 (1992);
M. Luo, p. 977 of Ref. 4.
255. F.S. Merritt *et al.*, p. 19 of *Particle Physics: Perspectives and Opportunities: Report of the DPF Committee on Long Term Planning*, ed. R. Peccei *et al.* (World Scientific, Singapore, 1995).
256. D.E. Morrissey, T. Plehn and T.M.P. Tait, [arXiv:0912.3259 \[hep-ph\]](#).
257. G. Altarelli, R. Barbieri, and S. Jadach, *Nucl. Phys.* **B369**, 3 (1992) and *ibid.*, **B376**, 444(E) (1992).
258. A. De Rújula *et al.*, *Nucl. Phys.* **B384**, 3 (1992);
K. Hagiwara *et al.*, *Phys. Rev.* **D48**, 2182 (1993);
C.P. Burgess *et al.*, *Phys. Rev.* **D49**, 6115 (1994);
Z. Han and W. Skiba, *Phys. Rev.* **D71**, 075009 (2005);
G. Cacciapaglia *et al.*, *Phys. Rev.* **D74**, 033011 (2006);
V. Bernard *et al.*, *JHEP* **0801**, 015 (2008);
Z. Han, *Int. J. Mod. Phys. A* **23**, 2653 (2008).
259. For reviews, see A. Leike, *Phys. Reports* **317**, 143 (1999);
P. Langacker, *Rev. Mod. Phys.* **81**, 1199 (2009).
260. M. Cvetič and P. Langacker, *Phys. Rev.* **D54**, 3570 (1996).
261. J. Erler, P. Langacker and T. Li, *Phys. Rev.* **D66**, 015002 (2002).
262. S. Chaudhuri *et al.*, *Nucl. Phys.* **B456**, 89 (1995);
G. Cleaver *et al.*, *Phys. Rev.* **D59**, 055005 (1999).
263. B. Holdom, *Phys. Lett.* **B166**, 196 (1986).
264. M. Carena *et al.*, *Phys. Rev.* **D70**, 093009 (2004).
265. J. Erler, P. Langacker, S. Munir and E. Rojas, *JHEP* **0908**, 017 (2009).
266. CDF: T. Aaltonen *et al.*, *Phys. Rev. Lett.* **102**, 091805 (2009).
267. M. Jaffré, presented at EPS-HEP 2009; see also www-d0.fnal.gov/Run2Physics/WWW/results
268. J. Kang and P. Langacker, *Phys. Rev.* **D71**, 035014 (2005).
269. T. Appelquist, B.A. Dobrescu, and A.R. Hopper, *Phys. Rev.* **D68**, 035012 (2003);
R.S. Chivukula *et al.*, *Phys. Rev.* **D69**, 015009 (2004).